

MULTILEVEL DIMENSION-INDEPENDENT LIKELIHOOD-INFORMED MCMC FOR LARGE-SCALE INVERSE PROBLEMS *

TIANGANG CUI[†], GIANLUCA DETOMMASO[‡], AND ROBERT SCHEICHL[§]

Abstract. We present a non-trivial integration of dimension-independent likelihood-informed (DILI) MCMC (Cui, Law, Marzouk, 2016) and the multilevel MCMC (Dodwell et al., 2015) to explore the hierarchy of posterior distributions. This integration offers several advantages: First, DILI-MCMC employs an intrinsic *likelihood-informed subspace* (LIS) (Cui et al., 2014) – which involves a number of forward and adjoint model simulations – to design accelerated operator-weighted proposals. By exploiting the multilevel structure of the discretised parameters and discretised forward models, we design a *Rayleigh-Ritz procedure* to significantly reduce the computational effort in building the LIS and operating with DILI proposals. Second, the resulting DILI-MCMC can drastically improve the sampling efficiency of MCMC at each level, and hence reduce the integration error of the multilevel algorithm for fixed CPU time. To be able to fully exploit the power of multilevel MCMC and to reduce the dependencies of samples on different levels for a parallel implementation, we also suggest a new pooling strategy for allocating computational resources across different levels and constructing Markov chains at higher levels conditioned on those simulated on lower levels. Numerical results confirm the improved computational efficiency of the multilevel DILI approach.

Key words. multilevel Monte Carlo, likelihood-informed subspaces, dimension independent MCMC, inverse problems

AMS subject classifications. 15A29, 65C05, 65C60

1. Introduction. Inverse problems aim to estimate unknown parameters of mathematical models from noisy and indirect observations. The unknown parameters, often represented as functions, are related to the observed data through a forward model, such as a differential equation, that maps realisations of parameters to observables. Due to smoothing properties of the forward model and incompleteness of data, such inverse problems are often ill-posed: there may exist many feasible realisations of parameters that are consistent with the observed data, and small perturbations in the data may lead to large perturbations in unregularised parameter estimates. The Bayesian approach [35, 24, 34] casts the solution of inverse problems as the posterior probability distribution of the model parameters conditioned on the data. This offers a natural way to integrate the forward model and the data together with prior knowledge and a stochastic description of measurement and/or model errors to remove the ill-posedness and to quantify uncertainties in parameters and parameter-dependent predictions. As a result, parameter estimations, model predictions, and associated uncertainty quantifications can be issued in the form of marginal distributions or expectations of some quantities of interest (QoI) over the posterior. Due to the typically high parameter dimensions and the high computational cost of the forward models, characterising the posterior and computing posterior expectations are in general computationally challenging tasks. Integrating multilevel Markov chain Monte Carlo (MCMC) [21, 13], likelihood-informed parameter reduction [11, 33, 39] and dimension-independent MCMC [4, 8, 10, 31], we present here an integrated framework to significantly accelerate the computation of posterior expectations for large-scale inverse problems.

In inverse problems, unknown parameters are often cast as functions, and hence the Bayesian inference has to be carried out over typically *high-dimensional discretisations* of the parameters that resolve the spatial and/or temporal variability of the underlying problem sufficiently. Examples are the permeability field of a porous medium [20, 9, 22, 13] or Brownian forcing of a stochastic ordinary differential equation [3]. In those settings, efficient MCMC

*Submitted to the editors DATE.

Funding: Funding information goes here.

[†]School of Mathematics, Monash University, Victoria 3800, Australia (tiangang.cui@monash.edu).

[‡]Department of Mathematical Sciences, University of Bath, Bath, BA2 7AY, UK (gd391@bath.ac.uk).

[§]Institute for Applied Mathematics and Interdisciplinary Center for Scientific Computing, Heidelberg University, Im Neuenheimer Feld 205, 69120 Heidelberg, Germany (r.scheichl@uni-heidelberg.de).

methods have been developed to sample the posterior and compute posterior expectations with convergence rates that are independent of the discretised parameter dimension: for example, (preconditioned) Crank-Nicolson (pCN) methods [4, 8, 18] that establish the foundation for designing and analysing MCMC algorithms in a function space setting, stochastic Newton methods [27, 29] that utilise Hessian information to accelerate the convergence, as well as operator-weighted methods [25, 10, 31] that generalise PCN methods using (potentially location-dependent) operators to adapt to the geometry of the posterior.

Discretisation also arises in the numerical simulation of the forward model, for instance, finite-element discretisations of PDEs. As many degrees of freedom are needed to accurately resolve the forward model, simulating the posterior density (which includes a forward model evaluation) can be computationally demanding. One natural way to reduce the computational cost is to utilise a hierarchy of forward models defined by a sequence of grid discretisations, ranging from computationally cheaper and less accurate coarse models to more costly but more accurate fine models. Corresponding to this hierarchy of models, the parameters can also be represented by a sequence of discretised functions with increasing dimensions. This yields a *hierarchy of posterior distributions*. By allocating different numbers of MCMC simulations to sample posteriors across different levels and by combining all those sample-based posterior estimations using a *telescoping sum* [14], the multilevel MCMC [21, 13] provides accelerated and unbiased estimates of posterior expectations.

We present a non-trivial integration of the dimension-independent likelihood-informed (DILI) MCMC [10] and the multilevel MCMC in [13] to explore the hierarchy of posterior distributions. This integration offers several advantages: First, DILI-MCMC employs an intrinsic *likelihood-informed subspace* (LIS) [11]—which involves a number of forward and adjoint model simulations—to design accelerated operator-weighted proposals. By exploiting the multilevel structure of the discretised parameters and discretised forward models, we design a *Rayleigh-Ritz procedure* to significantly reduce the computational effort in building a *hierarchical LIS* and operating with DILI proposals. Second, the resulting DILI-MCMC can drastically improve the sampling efficiency of MCMC at each level, and hence reduce the integration error of multilevel Monte Carlo for a fixed CPU time budget. To be able to fully exploit the power of multilevel MCMC and to reduce the dependencies of samples on different levels for a parallel implementation, we also suggest a new pooling strategy for allocating computational resources across different levels and constructing Markov chains at higher levels conditioned on those simulated on lower levels. Numerical results confirm the improved computational efficiency of the proposed multilevel DILI approach.

We note that the DILI proposal has been used before in the multilevel sequential Monte Carlo (SMC) setting [2], but in a very different way. We use derivative information of the likelihood to recursively construct the LIS via matrix-free eigenvalue solves, whereas [2] uses multilevel SMC to estimate the full-rank empirical posterior covariance matrix and then builds the LIS from this posterior covariance matrix. Moreover, we construct DILI proposals by exploiting the structure of the hierarchical LIS to couple Markov chains across levels, whereas [2] employs the original DILI proposal in the mutation step of SMC to improve mixing.

The paper is structured as follows. Section 2 introduces the framework of Bayesian inverse problems and MCMC sampling while section 3 discusses the general framework of multilevel MCMC. The Rayleigh-Ritz procedure for the recursive construction of the hierarchical LIS is presented in section 4. The new coupling strategy in the implementation of multilevel MCMC, as well as the coupled DILI proposals exploiting the hierarchical LIS are introduced in section 5. Section 6 provides numerical experiments to demonstrate the efficacy of the resulting MLDILI method, while finally, in section 7, we provide some concluding remarks.

2. Background. In this section, we review the Bayesian formulation of inverse problems, the dimension-independent likelihood-informed MCMC approach, posterior discretisation, as well as the bias-variance decomposition for MCMC algorithms.

2.1. Bayesian inference framework. Suppose the parameter of interest is some function u in a separable Hilbert space $\mathcal{H}(\Omega)$ defined over a given bounded domain $\Omega \subset \mathbb{R}^d$. We introduce a prior probability measure μ_0 satisfying $\mu_0(\mathcal{H}) = 1$ to represent the *a priori* information about the function u . The inner product on \mathcal{H} is denoted by $\langle \cdot, \cdot \rangle_{\mathcal{H}}$, with associated norm denoted by $\|\cdot\|_{\mathcal{H}}$. For brevity, where misinterpretation is not possible, we will drop the subscript \mathcal{H} . We assume that the prior measure is Gaussian with mean $m_0 \in \mathcal{H}$ and a self-adjoint, positive definite covariance operator Γ_{pr} that is trace-class, so that the prior provides a full probability measure on \mathcal{H} .

Given observed data $\mathbf{y} \in \mathbb{R}^d$ and the forward model $F : \mathcal{H} \rightarrow \mathbb{R}^d$, we define the likelihood function $\mathcal{L}(\mathbf{y}|u)$ of \mathbf{y} given u . Denoting the posterior probability measure by $\mu_{\mathbf{y}}$, the posterior distribution on any infinitesimal volume $du \in \mathcal{H}$ is given by

$$(2.1) \quad \mu_{\mathbf{y}}(du) \propto \mathcal{L}(\mathbf{y}|u)\mu_0(du).$$

Making the simplifying assumption that the observational noise is additive and Gaussian with zero mean and covariance matrix Γ_{obs} , the observation model has the form

$$(2.2) \quad \mathbf{y} = F(u) + \mathbf{e}, \quad \mathbf{e} \sim \mathcal{N}(0, \Gamma_{\text{obs}}),$$

and it follows immediately that the likelihood function satisfies

$$(2.3) \quad \mathcal{L}(\mathbf{y}|u) \propto \exp(-\eta(u; \mathbf{y})),$$

where $\eta(\mathbf{y}; u)$ is the data-misfit functional defined by

$$(2.4) \quad \eta(u; \mathbf{y}) \equiv \frac{1}{2}(\mathbf{y} - F(u))^\top \Gamma_{\text{obs}}^{-1}(\mathbf{y} - F(u)).$$

ASSUMPTION 2.1. *We assume that the forward model $F : \mathcal{H} \rightarrow \mathbb{R}^d$ satisfies:*

1. *For all $\varepsilon > 0$, there exists a constant $K(\varepsilon) > 0$ such that, for all $u \in \mathcal{H}$,*

$$|F(u)| \leq \exp(K(\varepsilon) + \varepsilon\|u\|_{\mathcal{H}}^2).$$

2. *For any $u \in \mathcal{H}$, there exists a bounded linear operator $J(u) : \mathcal{H} \rightarrow \mathbb{R}^d$ such that*

$$\lim_{\delta u \rightarrow 0} \frac{|F(u + \delta u) - F(u) - J(u)\delta u|}{\|\delta u\|_{\mathcal{H}}} = 0, \quad \forall \delta u \in \mathcal{H}.$$

In particular, this also implies the Lipschitz continuity of F .

Given observations \mathbf{y} such that $\|\mathbf{y}\| < \infty$ and a forward model that satisfies Assumption 2.1, [34] shows that the resulting data-misfit function is sufficiently bounded and locally Lipschitz, and thus the posterior measure is dominated by the prior measure. The second condition states that the forward model is first-order Fréchet differentiable, and hence the Gauss-Newton approximation of the Hessian of the data-misfit functional is bounded.

Suppose we have some quantity of interest (QoI) that is a functional of the parameter u denoted by $Q : \mathcal{H} \rightarrow \mathbb{R}^q$, e.g., flow rate. Then, posterior-based model predictions can be formulated as expectations of that QoI over the posterior. We will denote them by

$$\mathbb{E}_{\mu_{\mathbf{y}}}[Q] \equiv \mathbb{E}_{U \sim \mu_{\mathbf{y}}}[Q(U)].$$

MCMC methods draw (correlated) MCMC samples $U^{(1)}, \dots, U^{(N)}$ from the posterior and then estimate expected QoI(s) using Monte Carlo integration:

$$(2.5) \quad \mathbb{E}_{\mu_{\mathbf{y}}}[Q] \approx \frac{1}{N} \sum_{i=1}^N Q(U^{(i)}).$$

2.2. Dimension-independent likelihood-informed MCMC on function space.

The Metropolis-Hastings (MH) algorithm [28, 19] provides a general framework to design transition kernels that have the posterior as their invariant distribution to generate a Markov chain of random variables that targets the posterior.

DEFINITION 2.2 (Metropolis-Hastings Kernel). *Given the current state $U^{(k)} = u^*$, a candidate state u' is drawn from a proposal distribution $q(u^*, \cdot)$. The transition probability from $U^{(k)} = u^*$ to u' and the reverse transition probability are defined by the pair of measures*

$$(2.6) \quad \begin{aligned} \nu(du^*, du') &= q(u^*, du')\mu_y(du^*) \\ \nu^\perp(du^*, du') &= q(u', du^*)\mu_y(du'). \end{aligned}$$

Then, the next state of the Markov chain is set to $U^{(k+1)} = u'$ with probability

$$(2.7) \quad \alpha(u^*, u') = \min \left\{ 1, \frac{d\nu^\perp}{d\nu}(u^*, u') \right\},$$

and to $U^{(k+1)} = u^*$ otherwise.

MH algorithms require the absolute continuity condition $\nu^\perp \ll \nu$ to define a valid transition kernel with non-zero acceptance probability as the dimension goes to infinity [38]. We will refer to a MH algorithm as *well-defined* (and *dimension-independent*) if this absolute continuity condition holds. For probability measures over function spaces in the setting considered here, the sequence of papers [4, 34, 18, 8, 17] provide a viable way to construct well-defined MH algorithms using a preconditioned Crank-Nicolson (pCN) discretisation of a particular Langevin SDE. The pCN proposal has the form

$$(2.8) \quad u' = a(u^* - m_0) + m_0 - \gamma(1 - a)\Gamma_{\text{pr}}\nabla_u\eta(u^*; \mathbf{y}) + \sqrt{1 - a^2}\Gamma_{\text{pr}}^{\frac{1}{2}}\xi,$$

where $\xi \sim \mathcal{N}(0, I)$ and $\gamma \in \{0, 1\}$ is a tuning parameter to switch between Langevin ($\gamma = 1$) and Ornstein-Uhlenbeck proposal ($\gamma = 0$). It is required that $a \in (-1, 1)$. The pCN proposal (2.8) satisfies the desired absolute continuity condition and the acceptance probability does not go to zero as the discretisation of u is refined.

The pCN proposal (2.8) scales uniformly in all directions with respect to the norm induced by the prior covariance. Since the posterior necessarily contracts the prior along parameter directions that are informed by the likelihood, the Markov chain produced by the standard pCN proposal decorrelates more quickly in the likelihood-informed parameter subspace than in the orthogonal complement, which is prior-dominated [25, 10]. Thus, proposed moves of pCN can be effectively too small in prior-dominated directions, resulting in poor mixing.

The dimension-independent likelihood-informed (DILI) MCMC [10] provides a systematic way to design proposals that adapt to the anisotropic structure of the posterior while retaining dimension-independent performance. It considers operator-weighted proposals in the form of

$$(2.9) \quad u' = \Gamma_{\text{pr}}^{\frac{1}{2}}A\Gamma_{\text{pr}}^{-\frac{1}{2}}(u^* - m_0) + m_0 - \Gamma_{\text{pr}}^{\frac{1}{2}}G\Gamma_{\text{pr}}^{\frac{1}{2}}\nabla_u\eta(u^*; \mathbf{y}) + \Gamma_{\text{pr}}^{\frac{1}{2}}B\xi,$$

where A, B, and G are bounded, self-adjoint operators on $\text{Im}(\Gamma_{\text{pr}}^{-1/2})$ that satisfy certain properties to be discussed below. In this paper, we set G to zero throughout and thus consider only non-Langevin type proposals. By applying a whitening transform

$$(2.10) \quad v = \Gamma_{\text{pr}}^{-\frac{1}{2}}(u - m_0)$$

to the parameter u and by denoting (in a slight abuse of notation) the associated data-misfit functional again by $\eta(v; y) \leftarrow \eta(\Gamma_{\text{pr}}^{1/2}v + m_0; y)$, the proposal (2.9) simplifies to

$$(2.11) \quad v' = Av^* + B\xi.$$

The following theorem provides sufficient conditions for constructing the operators A and B such that the proposal (2.11) yields a well-defined MH algorithm, as well as a formula for the acceptance probability.

THEOREM 2.3. *Suppose that the posterior measure μ_y is equivalent to the prior measure μ_0 and that the self-adjoint operators A and B commute, that is, they can be defined by a common set of eigenfunctions $\{\psi_i \in \text{Im}(\Gamma_{\text{pr}}^{-1/2}) : i \in \mathbb{N}\}$ with corresponding eigenvalues $\{a_i\}_{i=1}^\infty$ and*

$\{b_i\}_{i=1}^\infty$, respectively. Suppose further that

$$\{a_i\}_{i=1}^\infty, \{b_i\}_{i=1}^\infty \subset \mathbb{R} \setminus \{0\} \quad \text{and} \quad \sum_{i=1}^\infty (a_i^2 + b_i^2 - 1)^2 < \infty.$$

Then, the proposal (2.11) delivers a well-defined MCMC algorithm and the acceptance probability is given by

$$\alpha(v^*, v') = \min \left\{ 1, \frac{\exp(-\eta(v'; y) - \frac{1}{2}(v', B^{-2}(A^2 + B^2 - I)v'))}{\exp(-\eta(v^*; y) - \frac{1}{2}(v^*, B^{-2}(A^2 + B^2 - I)v^*))} \right\}.$$

Proof. The above assumptions are simplified versions of those in Theorem 3.1 of [10]. The acceptance probability directly follows from Corollary 3.5 of [10]. \square

The DILI proposal (2.11) enables different scalings in the proposal moves along different parameter directions. By choosing appropriate eigenfunctions $\{\psi_i\}_{i=1}^\infty$ and eigenvalues $\{a_i, b_i\}_{i=1}^\infty$, it can capture the geometry of the posterior, and thus can potentially improve the mixing of the resulting Markov chain.

The likelihood-informed subspace (LIS) [11, 12] provides a viable way to construct such operators A and B. It is spanned by the leading eigenfunctions of the eigenvalue problem

$$(2.12) \quad \mathbb{E}_{V \sim \mu^*} [\mathbf{H}(V)] \psi_i = \lambda_i \psi_i,$$

where $\mathbf{H}(v)$ is some information metric of the likelihood function (with respect to the transformed parameter v), for example, the Hessian of the data-misfit functional or the Fisher information, and μ^* is some reference measure, for example, the posterior or the Laplace approximation of the posterior. In the LIS, spanned by $\{\psi_1, \dots, \psi_r\}$, the posterior may significantly differ from the prior. Thus, we prescribe inhomogeneous eigenvalues $\{a_i\}_{i=1}^r$ and $\{b_i\}_{i=1}^r$ to ensure that the proposal follows the possibly relatively tight geometry of the posterior. In the complement of the LIS, where the posterior does not differ significantly from the prior, we can use the original pCN proposal and set $\{a_i\}_{i>r}$ and $\{b_i\}_{i>r}$ to some constant values a_\perp and b_\perp , respectively. Further details on the computation of the LIS basis and the choice of eigenvalues will be discussed in the multilevel context in later sections.

2.3. Posterior discretisation and bias-variance decomposition. When the forward model involves a partial/ordinary differential equation and the parameter is defined as a spatial/temporal stochastic process, it is necessary in practice to discretise the parameter and the forward model using appropriate numerical methods.

A common way to discretise the parameter is the Karhunen–Loève expansion, which also serves the purpose of the whitening transform. Given the prior mean $m_0(x)$ and the prior covariance Γ_{pr} , we express the unknown parameter u as the linear combination of the first R eigenfunctions $\{\phi_1, \dots, \phi_R\}$ of the eigenvalue problem $\Gamma_{\text{pr}} \phi_j = \omega_j \phi_j$, such that

$$(2.13) \quad u_R(x) = m_0(x) + \sum_{j=1}^R \sqrt{\omega_j} \phi_j(x) v_j, \quad x \in \Omega.$$

The discretised prior $p_R(\mathbf{v})$ associated with the random coefficients $\mathbf{v} = [v_1, \dots, v_R]^\top$ is Gaussian with zero mean and covariance equal to the $R \times R$ identity matrix \mathbf{I}_R .

We discretise the forward model using a numerical method, such as finite elements or finite differences, with M degrees of freedom, which yields a discretised forward model $F_{R,M}$ mapping from the discretised coefficients \mathbf{v} to the observables. In this way, the posterior measure (2.1) can be discretised, leading to the discrete density

$$(2.14) \quad \pi_{R,M}(\mathbf{v}|\mathbf{y}) \propto \exp(-\eta_{R,M}(\mathbf{v}; \mathbf{y})) p_R(\mathbf{v}),$$

where

$$\eta_{R,M}(\mathbf{v}; \mathbf{y}) = \frac{1}{2} (\mathbf{y} - F_{R,M}(\mathbf{v}))^\top \Gamma_{\text{obs}}^{-1} (\mathbf{y} - F_{R,M}(\mathbf{v}))$$

is the discretised data-misfit function. Correspondingly, we also define the discretised QoI $Q_{R,M}(\mathbf{v})$, which maps the discretise coefficient vector \mathbf{v} to the discretised QoI.

The discretised parameters and forward models can be indexed by the discretisation level. We consider a hierarchy of $L + 1$ levels of discretised parameter spaces with dimensions $R_0 \leq R_1 \leq \dots \leq R_L$ and a hierarchy of discretised forward models with $M_0 \leq M_1 \leq \dots \leq M_L$ degrees of freedom. Discretised parameter, forward model and QoI on level ℓ are denoted by

$$\mathbf{v}_\ell = [v_1, \dots, v_{R_\ell}]^\top, \quad F_\ell(\mathbf{v}_\ell) \equiv F_{R_\ell, M_\ell}(\mathbf{v}_\ell) \quad \text{and} \quad Q_\ell(\mathbf{v}_\ell) \equiv Q_{R_\ell, M_\ell}(\mathbf{v}_\ell),$$

respectively. Thus, the discretised data-misfit function, prior and posterior on level ℓ are

$$(2.15) \quad \eta_\ell(\mathbf{v}_\ell; \mathbf{y}) \equiv \eta_{R_\ell, M_\ell}(\mathbf{v}_\ell; \mathbf{y}), \quad p_\ell(\mathbf{v}_\ell) \equiv p_{R_\ell}(\mathbf{v}_\ell), \quad \text{and} \quad \pi_\ell(\mathbf{v}_\ell | \mathbf{y}) \equiv \pi_{R_\ell, M_\ell}(\mathbf{v}_\ell | \mathbf{y}),$$

respectively, with the associated posterior expectation $\mathbb{E}_{\pi_\ell}[Q_\ell] \equiv \mathbb{E}_{\mathbf{v}_\ell \sim \pi_\ell}[Q_\ell(\mathbf{V}_\ell)]$.

ASSUMPTION 2.4. (i) *The bias of the posterior expectation on level ℓ can be bounded in terms of the number of degrees of freedom of the forward model such that*

$$(2.16) \quad |\mathbb{E}_{\mu_y}[Q] - \mathbb{E}_{\pi_\ell}[Q_\ell]| = \mathcal{O}(M_\ell^{-\vartheta_b}),$$

for some constant $\vartheta_b > 0$. Implicitly, this assumes that R_ℓ is sufficiently large such that the bias due to parameter approximation is dominated by the error due to the forward model approximation on level ℓ .

(ii) *For the computational cost of carrying out one step of MCMC (including a forward model simulation) it is assumed that there exists a constant $\vartheta_c > 0$ such that*

$$(2.17) \quad C_\ell = \mathcal{O}(M_\ell^{\vartheta_c}).$$

Consider discretisation level L and let $\{\mathbf{V}_L^{(j)}\}_{j=1}^{N_{MC}}$ be a Markov chain produced by a MCMC algorithm converging in distribution to π_L . An estimate for the expectation $\mathbb{E}_{\pi_L}[Q_L]$ is

$$(2.18) \quad Y^{MC} \equiv \frac{1}{N_{MC}} \sum_{j=1}^{N_{MC}} Q_L(\mathbf{V}_L^{(j)}) \approx \mathbb{E}_{\pi_L}[Q_L].$$

The mean-squared-error (MSE) of the Monte Carlo estimator (2.18) allows a bias-variance decomposition of the form

$$(2.19) \quad \text{MSE}(Y^{MC}) = \underbrace{\left| \mathbb{E}_{\mu_y}[Q] - \mathbb{E}_{\pi_L}[Q_L] \right|^2}_{\text{Square of Bias}} + \underbrace{\text{Var}_{\pi_L}(Q_L)}_{\text{Var}(Y^{MC})} / N_{MC}^{\text{eff}},$$

where N_{MC}^{eff} is the effective sample size of the Markov chain $\{\mathbf{V}_L^{(j)}\}_{j=1}^{N_{MC}}$. This effective sample size is proportional to the total sample size, i.e., $N_{MC}^{\text{eff}} = N_{MC} / \tau_{MC}$, where $\tau_{MC} \geq 1$ is the integrated autocorrelation time (IACT) of the Markov chain.

Choosing N_{MC} such that the two terms in (2.19) of the MCMC estimator are balanced and using Assumption 2.4, the total computational cost to achieve $\text{MSE}(Y^{MC}) < \varepsilon^2$ is

$$(2.20) \quad C^{MC} = \mathcal{O}(\tau_{MC} \varepsilon^{-2 - \vartheta_c / \vartheta_b}).$$

Thus, one of the key aims in accelerating MCMC sampling is to reduce the IACT. This will be achieved via the DILI MCMC proposal. However, the multilevel method will allow us to also improve on the asymptotic rate for the cost of the standard MCMC estimator in (2.20).

3. Multilevel MCMC. By exploiting the hierarchy of posteriors, the rate of the computational cost in (2.20) can be reduced significantly using the multilevel idea in [13]. We expand the posterior expectation in the telescoping sum

$$(3.1) \quad \mathbb{E}_{\pi_L}[Q_L] = \mathbb{E}_{\pi_0}[Q_0] + \sum_{\ell=1}^L \left(\mathbb{E}_{\pi_\ell}[Q_\ell] - \mathbb{E}_{\pi_{\ell-1}}[Q_{\ell-1}] \right).$$

For level zero, the sample set $\{\mathbf{V}_0^{(0,j)}\}_{j=1}^{N_0}$ is assumed to be drawn via some MCMC method that converges to $\pi_0(\cdot|\mathbf{y})$ and the first term in the telescoping sum (3.1) is estimated via

$$Y_0 \equiv \frac{1}{N_0} \sum_{j=1}^{N_0} D_0^{(j)} \approx \mathbb{E}_{\pi_0}[Q_0], \quad \text{where } D_0^{(j)} = Q_0(\mathbf{V}_0^{(0,j)}).$$

Since the two expectations in the difference $\mathbb{E}_{\pi_\ell}[Q_\ell] - \mathbb{E}_{\pi_{\ell-1}}[Q_{\ell-1}]$ are with respect to different discretisations of the posterior, special treatment is required for $\ell > 0$. Let $\Delta_{\ell,\ell-1}(\mathbf{v}_\ell, \mathbf{v}_{\ell-1})$ be the joint density of \mathbf{v}_ℓ and $\mathbf{v}_{\ell-1}$ such that

$$(3.2) \quad \int \Delta_{\ell,\ell-1}(\mathbf{v}_\ell, \mathbf{v}_{\ell-1}) d\mathbf{v}_{\ell-1} = \pi_\ell(\mathbf{v}_\ell|\mathbf{y}) \quad \text{and} \quad \int \Delta_{\ell,\ell-1}(\mathbf{v}_\ell, \mathbf{v}_{\ell-1}) d\mathbf{v}_\ell = \pi_{\ell-1}(\mathbf{v}_{\ell-1}|\mathbf{y}),$$

that is, the posteriors $\pi_\ell(\mathbf{v}_\ell|\mathbf{y})$ and $\pi_{\ell-1}(\mathbf{v}_{\ell-1}|\mathbf{y})$ are the two marginals. Then, the difference between expectations can be expressed as

$$(3.3) \quad \mathbb{E}_{\pi_\ell}[Q_\ell] - \mathbb{E}_{\pi_{\ell-1}}[Q_{\ell-1}] = \mathbb{E}_{\Delta_{\ell,\ell-1}}[D_\ell], \quad \text{where } D_\ell = Q_\ell(\mathbf{V}_\ell) - Q_{\ell-1}(\mathbf{V}_{\ell-1})$$

and $(\mathbf{V}_\ell, \mathbf{V}_{\ell-1}) \sim \Delta_{\ell,\ell-1}(\cdot, \cdot)$. The construction of the joint density and the associated sampling procedure will be critical to reduce the computational complexity.

Suppose the samples $\{(\mathbf{V}_\ell^{(\ell,j)}, \mathbf{V}_{\ell-1}^{(\ell,j)})\}_{j=1}^{N_\ell}$ form a Markov chain that converges in distribution to $\Delta_{\ell,\ell-1}(\cdot, \cdot)$ and

$$D_\ell^{(j)} = Q_\ell(\mathbf{V}_\ell^{(\ell,j)}) - Q_{\ell-1}(\mathbf{V}_{\ell-1}^{(\ell,j)}).$$

Then, the remaining terms in (3.1), for $\ell = 1, \dots, L$, are estimated by

$$Y_\ell \equiv \frac{1}{N_\ell} \sum_{j=1}^{N_\ell} D_\ell^{(j)} \approx \mathbb{E}_{\pi_\ell}[Q_\ell] - \mathbb{E}_{\pi_{\ell-1}}[Q_{\ell-1}]$$

and the multilevel MCMC estimator for $\mathbb{E}_{\pi_L}[Q_L]$ is defined by

$$(3.4) \quad \mathbb{E}_{\pi_L}[Q_L] \approx Y^{\text{ML}} \equiv \sum_{\ell=0}^L Y_\ell,$$

The mean square error of this estimator can again be decomposed as follows:

$$(3.5) \quad \text{MSE}(Y^{\text{ML}}) \equiv \underbrace{|\mathbb{E}_{\mu_y}[Q] - \mathbb{E}_{\pi_L}[Q_L]|^2}_{\text{Square of Bias}} + \underbrace{\sum_{\ell=0}^L (\text{Var}(Y_\ell) + \sum_{k \neq \ell}^L \text{Cov}(Y_\ell, Y_k))}_{\text{Var}(Y^{\text{ML}})}.$$

3.1. Variance management. For optimal efficiency, we now choose the numbers of samples N_ℓ , $\ell = 0, \dots, N$, such as to minimise $\text{Var}(Y^{\text{ML}})$ for fixed computational effort. This includes the *within-level variance* $\text{Var}(Y_\ell)$ and the *cross-level variance* $\text{Cov}(Y_\ell, Y_k)$ for $k \neq \ell$. We will provide justifications on managing these variances using the following assumptions.

ASSUMPTION 3.1. *The Markov chains on all levels are assumed to be ergodic. This implies that the effective sample sizes are proportional to the total sample sizes, i.e., $N_\ell^{\text{eff}} = N_\ell/\tau_\ell$, for all ℓ , where $\tau_\ell \geq 1$ is the IACT of the Markov chain $D_\ell^{(j)}$.*

Remark 3.2. The ergodicity in Assumption 3.1 can be satisfied by removing burn-in samples using shorter MCMC simulations. The within-level variance has the form

$$(3.6) \quad \text{Var}(Y_\ell) = \frac{1}{N_\ell^{\text{eff}}} \text{Var}_{\Delta_{\ell,\ell-1}}(D_\ell) = \frac{\tau_\ell}{N_\ell} \text{Var}_{\Delta_{\ell,\ell-1}}(D_\ell),$$

where we set $\text{Var}_{\Delta_{0,-1}}(D_0) = \text{Var}_{\pi_0}(Q_0)$ and have

$$\text{Var}_{\Delta_{\ell,\ell-1}}(D_\ell) = \text{Var}_{\pi_\ell}(Q_\ell) + \text{Var}_{\pi_{\ell-1}}(Q_{\ell-1}) - 2\text{Cov}_{\Delta_{\ell,\ell-1}}(Q_\ell, Q_{\ell-1}) \geq 0, \quad \forall \ell > 0,$$

by Cauchy–Schwarz inequality. Thus, to reduce $\text{Var}(Y_\ell)$, the joint density should be constructed in such a way that $\text{Cov}_{\Delta_{\ell,\ell-1}}(Q_\ell, Q_{\ell-1})$ is *positive* and (if possible) maximised. In addition, the MCMC simulation should be made *statistically efficient* in the sense that τ_ℓ is as close to one as possible.

ASSUMPTION 3.3. *The variance $\text{Var}_{\Delta_{\ell,\ell-1}}(D_\ell)$ converges to zero as $M_\ell \rightarrow \infty$ and*

$$(3.7) \quad \text{Var}_{\Delta_{\ell,\ell-1}}(D_\ell) = \mathcal{O}(M_\ell^{-\vartheta_v}),$$

for some constant $\vartheta_v > 0$.

PROPOSITION 3.4. *Suppose that there exists an $r < 1$ such that*

$$(3.8) \quad \frac{\text{Cov}(Y_\ell, Y_k)}{\max\{\text{Var}(Y_\ell), \text{Var}(Y_k)\}} \leq r^{|k-\ell|}, \quad \text{for all } k \neq \ell,$$

i.e., the cross-level covariance is insignificant compared to the within-level variance. Then

$$(3.9) \quad \text{Var}(Y^{\text{ML}}) = \sum_{\ell=0}^L \left(\text{Var}(Y_\ell) + \sum_{k \neq \ell}^L \text{Cov}(Y_\ell, Y_k) \right) \leq \frac{1+r}{1-r} \sum_{\ell=0}^L \text{Var}(Y_\ell).$$

Proof. Without loss of generality, we can assume the variances $\{\text{Var}(Y_\ell)\}_{\ell=0}^L$ are ordered as $\text{Var}(Y_\ell) \geq \text{Var}(Y_k)$ for $\ell < k$. Then we have the bound

$$\begin{aligned} \text{Var}(Y^{\text{ML}}) &= \sum_{\ell=0}^L \left(\text{Var}(Y_\ell) + 2 \sum_{k>\ell}^L \text{Cov}(Y_\ell, Y_k) \right) \\ &\leq \sum_{\ell=0}^L \text{Var}(Y_\ell) \left(1 + 2 \sum_{k>\ell}^{\infty} \frac{\text{Cov}(Y_\ell, Y_k)}{\text{Var}(Y_\ell)} \right) \\ &\leq \sum_{\ell=0}^L \text{Var}(Y_\ell) \left(1 + 2 \sum_{k>\ell}^{\infty} r^{(k-\ell)} \right) = \frac{1+r}{1-r} \sum_{\ell=0}^L \text{Var}(Y_\ell). \quad \square \end{aligned}$$

Using Proposition 3.4 and (3.6), the variance of the multilevel estimator satisfies

$$\text{Var}(Y^{\text{ML}}) = \mathcal{O} \left(\sum_{\ell=0}^L \frac{\tau_\ell}{N_\ell} \text{Var}_{\Delta_{\ell,\ell-1}}(D_\ell) \right).$$

The total computational cost is $C^{\text{ML}} = \sum_{\ell=0}^L N_\ell C_\ell$. This way, for a fixed variance, the computational cost is minimised by choosing the sample size

$$(3.10) \quad N_\ell \propto \sqrt{\tau_\ell \text{Var}_{\Delta_{\ell,\ell-1}}(D_\ell) / C_\ell},$$

which leads to a total computational cost that satisfies

$$(3.11) \quad C^{\text{ML}} \propto \sum_{\ell=0}^L \sqrt{\tau_\ell C_\ell \text{Var}_{\Delta_{\ell,\ell-1}}(D_\ell)}.$$

THEOREM 3.5. *For the multilevel MCMC estimator to satisfy $\text{MSE}(Y^{\text{ML}}) < \varepsilon^2$, the multilevel MCMC with N_ℓ chosen as in (3.10) requires an overall computational cost*

$$(3.12) \quad C^{\text{ML}} = \begin{cases} \mathcal{O}(\varepsilon^{-2}) & \text{if } \vartheta_v > \vartheta_c \\ \mathcal{O}(\varepsilon^{-2} |\log \varepsilon|^2) & \text{if } \vartheta_v = \vartheta_c \\ \mathcal{O}(\varepsilon^{-2 - (\vartheta_c - \vartheta_v) / \vartheta_b}) & \text{if } \vartheta_v < \vartheta_c \end{cases}.$$

Proof. Given Assumptions 2.4, 3.1, 3.3, and Proposition 3.4, this result directly follows from the complexity theorems for multilevel Monte Carlo in [14, 7]. \square

It is difficult to rigorously verify Assumption (3.8) in Proposition 3.4. However, it is often observed that the cross-level variance $\text{Cov}(Y_\ell, Y_k)$ rapidly decays to zero in practice, as the Markov chains used for computing Y_ℓ and Y_k with $\ell \neq k$ are statistically independent. For example, independent Markov chains are constructed in [23] and a subsampling strategy of coarse chains are employed in [13] to ensure independence. Under this assumption, we are able

to reduce the bound on the computational complexity of multilevel MCMC compared to that presented in [13], which has an extra $|\log \varepsilon|$ factor. For any positive values of ϑ_b, ϑ_v and ϑ_c , the multilevel MCMC approach asymptotically requires less computational effort than single-level MCMC. To choose optimal numbers of samples on the various levels, estimates of the IACTs τ_ℓ , of the variances $\text{Var}_{\Delta_{\ell, \ell-1}}(D_\ell)$, and of the computational costs C_ℓ are needed. Such quantities may not be known *a priori*, but they can all be obtained and adaptively improved (on the fly) as the simulation progresses.

3.2. Notations. To map vectors and matrices across adjacent levels of discretisation we define the following notation. Given the canonical basis $(\hat{e}_1, \hat{e}_2, \dots, \hat{e}_{R_\ell})$ of the parameter space at level ℓ , where $\hat{e}_j \in \mathbb{R}^{R_\ell}$, we define the basis matrices $\Theta_{\ell, c} \equiv (\hat{e}_1, \hat{e}_2, \dots, \hat{e}_{R_{\ell-1}})$ and $\Theta_{\ell, f} \equiv (\hat{e}_{R_{\ell-1}+1}, \dots, \hat{e}_{R_\ell})$, which correspond to the parameter coefficients ‘active’ at level $\ell-1$ and the additional coefficients. We can split the parameter \mathbf{v}_ℓ into two components

$$(3.13) \quad \mathbf{v}_\ell = \begin{bmatrix} \mathbf{v}_{\ell, c} \\ \mathbf{v}_{\ell, f} \end{bmatrix}, \quad \text{where } \mathbf{v}_{\ell, c} = \Theta_{\ell, c}^\top \mathbf{v}_\ell \text{ and } \mathbf{v}_{\ell, f} = \Theta_{\ell, f}^\top \mathbf{v}_\ell,$$

which correspond to the coefficients on the previous level $\ell-1$ and the additional coefficients. Given a matrix $A_\ell \in \mathbb{R}^{R_\ell \times R_\ell}$, we partition the matrix as

$$(3.14) \quad A_\ell = \begin{bmatrix} A_{\ell, cc} & A_{\ell, cf} \\ A_{\ell, fc} & A_{\ell, ff} \end{bmatrix},$$

where $A_{\ell, cc} \equiv \Theta_{\ell, c}^\top A_\ell \Theta_{\ell, c}$ and $A_{\ell, ff}, A_{\ell, fc}$ and $A_{\ell, cf}$ are defined analogously. The matrices $\Theta_{\ell, c}$ and $\Theta_{\ell, f}$ are never constructed explicitly. Operations with those matrices only involve the selection of the corresponding rows or columns of the matrix or vector.

4. Multilevel LIS. In this section, we develop a Rayleigh-Ritz procedure to recursively compute multilevel likelihood-informed subspaces. The resulting hierarchical LIS basis can be used to generalise DILI proposals to the multilevel setting and to improve the efficiency of multilevel MCMC sampling.

For each level $\ell \in \{0, 1, \dots, L\}$, we denote the linearisation of the forward model F_ℓ at a given parameter \mathbf{v}_ℓ by

$$J_\ell(\mathbf{v}_\ell) = \nabla_{\mathbf{v}_\ell} F_\ell(\mathbf{v}_\ell).$$

This yields the Gauss-Newton approximation of the Hessian of the data-misfit functional at \mathbf{v}_ℓ (hereafter referred to as the GNH) in the form of

$$(4.1) \quad H_\ell(\mathbf{v}_\ell) = J_\ell(\mathbf{v}_\ell)^\top \Gamma_{\text{obs}}^{-1} J_\ell(\mathbf{v}_\ell).$$

Commonly used in optimisation and regression, the GNH measures local sensitivity of the parameter-to-likelihood map. The leading eigenvectors of $H_\ell(\mathbf{v}_\ell)$ (corresponding to the largest eigenvalues) indicate parameter directions along which the likelihood function varies rapidly.

To measure the global sensitivity of the parameter-to-likelihood map, we compute the expectation of the local GNH matrix $H_\ell(\mathbf{v}_\ell)$ over some reference distribution $p_\ell^*(\mathbf{v}_\ell)$:

$$(4.2) \quad \mathbb{E}_{\mathbf{V}_\ell \sim p_\ell^*} [H_\ell(\mathbf{V}_\ell)].$$

We approximate the above expectation using the sample average with K_ℓ random samples drawn from the reference distribution, which yields

$$(4.3) \quad \mathbb{E}_{\mathbf{V}_\ell \sim p_\ell^*} [H_\ell(\mathbf{V}_\ell)] \approx \hat{H}_\ell \equiv \frac{1}{K_\ell} \sum_{k=1}^{K_\ell} H_\ell(\mathbf{v}_\ell^{(k)}), \quad \text{where } \mathbf{v}_\ell^{(k)} \sim p_\ell^*(\cdot).$$

Note that the matrix \hat{H}_ℓ is symmetric and positive semidefinite. Different choices of the reference distribution, such as the prior or the posterior, lead to different ways to construct the LIS and different performance characteristics.

Remark 4.1. Following the discussion in [12, 39], using the posterior as the reference leads to sharp approximation properties [39] compared to other choices. However, the posterior exploration relies on MCMC sampling, and thus this choice requires adaptively estimating LIS during the MCMC sampling. The Laplace approximation to the posterior provides a reasonable alternative in a wide range of problems where the posterior is unimodal. We use the Laplace approximation as the reference distribution in this work.

The choice of the reference distribution can have an impact on the quality of the LIS basis and on the IACT of the Markov chains produced by DILI MCMC, but it does not affect the convergence of MCMC, as DILI samples the full parameter space and only uses the LIS to reduce the IACT and thus to accelerate posterior sampling.

It is often computationally infeasible to explicitly form the GNH matrix (4.1). However, all we need are matrix-vector-products (MVPs) with the GNH matrix. This requires only applications of the linearised forward model $J_\ell(\mathbf{v}_\ell)$ and its adjoint $J_\ell(\mathbf{v}_\ell)^\top$, which are well-established operations in the PDE-constraint optimisation literature. We refer the readers to recent applications in Bayesian inverse problems for further details, e.g., [5, 27, 29].

4.1. Base level LIS. At the base level, we use the samples $\{\mathbf{v}_0^{(k)}\}_{k=1}^{K_0}$ drawn from the reference $p_0^*(\cdot)$ to construct the sample-averaged GNH, \widehat{H}_0 . Then, we use the Rayleigh quotient $\langle \phi, \widehat{H}_\ell \phi \rangle / \langle \phi, \phi \rangle$ to measure the (quadratic) change in the parameter-to-likelihood map along a parameter direction ϕ . Hence, the LIS can be identified via a sequence of optimisation problems of the form

$$(4.4) \quad \psi_{0,k+1} = \arg \max_{\|\phi\|=1} \langle \phi, \widehat{H}_0 \phi \rangle, \quad \text{subject to } \langle \phi, \psi_{0,i} \rangle = 0, \quad \text{for } i = 1, \dots, k,$$

where $\psi_{0,1}$ is the solution to the unconstrained optimisation problem. The sequence of optimisation problems in (4.4) is equivalent to finding the leading eigenvectors of \widehat{H}_0 .

DEFINITION 4.2 (Base level LIS). *Given the sample-averaged GNH \widehat{H}_0 on level 0 and a threshold $\varrho > 0$, we solve the eigenproblem*

$$(4.5) \quad \widehat{H}_0 \psi_{0,i} = \lambda_{0,i} \psi_{0,i},$$

and then use the r_0 leading eigenvectors with eigenvalues $\lambda_{0,i} > \varrho$, for $i = 1, \dots, r_0$, to define the LIS basis $\Psi_{0,r_0} = [\psi_{0,1}, \psi_{0,2}, \dots, \psi_{0,r_0}]$, which spans an r_0 -dimensional subspace in \mathbb{R}_0^R .

The eigenvalues in (4.5) provide empirical sensitivity measures of the likelihood function relative to the prior (which here is i.i.d. Gaussian) along corresponding eigenvectors [11, 39]. Eigenvectors corresponding to eigenvalues less than 1 can be interpreted as parameter directions where the likelihood is dominated by the prior. Thus, we typically choose a value less than one for the truncation threshold, i.e., $\varrho < 1$.

4.2. LIS enrichment. Because the computational cost of a MVP with the GNH scales at least linearly with the degrees of freedom M_ℓ of the forward model on level ℓ , constructing the LIS can be computationally costly. We present a new approach to accelerate the LIS construction by employing a *recursive LIS enrichment* using the hierarchy of forward models and parameter discretisations. The resulting hierarchy of LISs will be used to reduce the computational complexity of constructing and operating with the resulting DILI proposals.

We reuse the LIS bases computed on the coarser levels by 'lifting' them and then recursively enrich them at each new level using a *Rayleigh-Ritz procedure*, rather than recomputing the entire basis from scratch on each level. Ideally, the subspace added on each level will have decreasing dimension, as the model and parameter approximations were assumed to converge with $\ell \rightarrow \infty$ and thus no longer provide additional information for the parameter inference.

DEFINITION 4.3 (Lifted LIS basis). *Suppose we have an orthogonal LIS basis $\Psi_{\ell-1,r} \in \mathbb{R}^{R_{\ell-1} \times r_{\ell-1}}$ on level $\ell-1$. We lift $\Psi_{\ell-1,r}$ from the coarse parameter space $\mathbb{R}^{R_{\ell-1}}$ to the fine*

parameter space \mathbb{R}^{R_ℓ} using the basis matrix $\Theta_{\ell,c}$ defined in Section 3.2. The lifted LIS basis vectors are collect in the matrix

$$(4.6) \quad \Psi_{\ell,c} = \Theta_{\ell,c} \Psi_{\ell-1,r}.$$

PROPOSITION 4.4. *The lifted LIS basis matrix $\Psi_{\ell,c}$ has orthonormal columns that span an $r_{\ell-1}$ -dimensional subspace in \mathbb{R}^{R_ℓ} , i.e., $\Psi_{\ell,c}^\top \Psi_{\ell,c} = \mathbf{I}_{r_{\ell-1}}$.*

Proof. The proof directly follows as the matrix $\Theta_{\ell,c}$ has orthonormal columns. \square

Given K_ℓ samples $\{\boldsymbol{\psi}_\ell^{(k)}\}_{k=1}^{K_\ell}$ from the reference distribution $p_\ell^*(\cdot)$, let $\widehat{\mathbf{H}}_\ell$ be the resulting sample-averaged GNH. To enrich the lifted LIS basis $\Psi_{\ell,c}$ we now identify likelihood-sensitive parameter directions in the null space $\text{null}(\Psi_{\ell,c})$ by recursively optimising the Rayleigh quotient in the orthogonal complement of $\text{range}(\Psi_{\ell,c})$, i.e.,

$$(4.7) \quad \boldsymbol{\psi}_{\ell,k+1} = \arg \max_{\|\boldsymbol{\phi}\|=1} \langle \boldsymbol{\phi}, \widehat{\mathbf{H}}_\ell \boldsymbol{\phi} \rangle,$$

subject to $\Pi_{\ell,c} \boldsymbol{\phi} = 0$ and $\langle \boldsymbol{\phi}, \boldsymbol{\psi}_{\ell,i} \rangle = 0$, for $i = 1, \dots, k$,

where $\Pi_{\ell,c} = \Psi_{\ell,c} \Psi_{\ell,c}^\top$ is an orthogonal projector. This optimisation problem can be solved as an eigenvalue problem using the *Rayleigh-Ritz procedure* [32].

THEOREM 4.5. *The optimisation problem (4.7) is equivalent to finding the leading eigenvectors of the projected eigenproblem*

$$(4.8) \quad (\mathbf{I}_{R_\ell} - \Pi_{\ell,c}) \widehat{\mathbf{H}}_\ell \boldsymbol{\psi}_{\ell,i} = \gamma_{\ell,i} \boldsymbol{\psi}_{\ell,i}, \quad \|\boldsymbol{\psi}_{\ell,i}\| = 1.$$

Proof. This result follows from the properties of orthogonal projectors and of the stationary points of the Rayleigh quotient. Here, we sketch the proof as follows. The constraint $\Pi_{\ell,c} \boldsymbol{\phi} = 0$ implies $\boldsymbol{\phi} = (\mathbf{I}_{R_\ell} - \Pi_{\ell,c}) \boldsymbol{\phi}$, since $(\mathbf{I}_{R_\ell} - \Pi_{\ell,c})$ is also an orthogonal projector. Hence, the optimisation problem becomes

$$\boldsymbol{\psi}_{\ell,k+1} = \arg \max_{\|\boldsymbol{\phi}\|=1} \langle \boldsymbol{\phi}, (\mathbf{I}_{R_\ell} - \Pi_{\ell,c}) \widehat{\mathbf{H}}_\ell (\mathbf{I}_{R_\ell} - \Pi_{\ell,c}) \boldsymbol{\phi} \rangle, \quad \text{subject to } \langle \boldsymbol{\phi}, \boldsymbol{\psi}_{\ell,i} \rangle = 0, \quad i = 1, \dots, k.$$

The solutions (for $k = 1, 2, \dots$) to these optimisation problems are given by the leading eigenvectors of the eigenproblem

$$(\mathbf{I}_{R_\ell} - \Pi_{\ell,c}) \widehat{\mathbf{H}}_\ell (\mathbf{I}_{R_\ell} - \Pi_{\ell,c}) \boldsymbol{\psi}_{\ell,i} = \gamma_{\ell,i} \boldsymbol{\psi}_{\ell,i}.$$

However, since $\boldsymbol{\psi}_{\ell,i} \in \text{range}(\mathbf{I}_{R_\ell} - \Pi_{\ell,c})$ this is equivalent to

$$(\mathbf{I}_{R_\ell} - \Pi_{\ell,c}) \widehat{\mathbf{H}}_\ell \boldsymbol{\psi}_{\ell,i} = \gamma_{\ell,i} \boldsymbol{\psi}_{\ell,i}. \quad \square$$

DEFINITION 4.6 (LIS enrichment on level ℓ). *The leading s_ℓ (normalised) eigenvectors of the eigenproblem (4.8) with eigenvalues $\gamma_{\ell,i} > \rho$ are denoted by*

$$(4.9) \quad \Psi_{\ell,f} = [\boldsymbol{\psi}_{\ell,1}, \dots, \boldsymbol{\psi}_{\ell,s_\ell}].$$

They are added to the lifted LIS basis from level $\ell-1$ to form the enriched LIS basis

$$(4.10) \quad \Psi_{\ell,r} = [\Psi_{\ell,c}, \Psi_{\ell,f}]$$

on level ℓ , where the basis vectors in (4.9) denote the auxiliary ‘‘fine scale’’ directions added on level ℓ . By construction, all the LIS basis vectors at level ℓ are mutually orthogonal. That is, $\Psi_{\ell,r}^\top \Psi_{\ell,r} = \mathbf{I}_{r_\ell}$. We also have $r_\ell = r_{\ell-1} + s_\ell$.

4.3. Computational complexity. By construction, the LIS basis $\Psi_{\ell,r}$ is block upper triangular and can be recursively defined as

$$(4.11) \quad \Psi_{\ell,r} = [\Psi_{\ell,c}, \Psi_{\ell,f}] = \begin{bmatrix} \Psi_{\ell-1,r} & \mathbf{Z}_{\ell,c} \\ \mathbf{0} & \mathbf{Z}_{\ell,f} \end{bmatrix},$$

where $Z_{\ell,c} = \Theta_{\ell,c}^\top \Psi_{\ell,f} \in \mathbb{R}^{R_{\ell-1} \times s_\ell}$, $Z_{\ell,f} = \Theta_{\ell,f}^\top \Psi_{\ell,f} \in \mathbb{R}^{(R_\ell - R_{\ell-1}) \times s_\ell}$, and $\Psi_{\ell-1,r} \in \mathbb{R}^{R_{\ell-1} \times r_{\ell-1}}$. We have $s_\ell = r_\ell - r_{\ell-1}$ and define $s_0 = r_0$ for consistency. The hierarchical LIS reduces the computational cost of operating with the LIS basis and the associated storage cost. This is critical for building efficient multilevel DILI proposals that will be discussed later. In addition, the recursive LIS enrichment is computationally more efficient, since the amount of costly PDE solves on the finer levels will be significantly reduced. Here we analyse and compare the complexities of the construction of the hierarchical LIS and of the single-level LIS, constructed directly on level L .

We analyse the construction of the hierarchical LIS under the following assumptions.

- ASSUMPTION 4.7. 1. *The parameter dimensions satisfy $R_\ell = R_0 e^{\beta_p \ell}$ for some $\beta_p > 0$.*
 2. *The number of auxiliary LIS basis vectors satisfies $s_\ell \leq s_0 e^{-\beta_s \ell}$ for some $\beta_s > 0$.*
 3. *The degrees of freedom in the forward model satisfy $M_\ell = M_0 e^{\beta_m \ell}$ for some $\beta_m > 0$.*
 4. *The computational cost of a MVP with one sample of the GNH $\mathbf{H}_\ell(\mathbf{v}_\ell^{(k)})$ is proportional to one evaluation of the forward model and thus $\mathcal{O}(M_\ell^{\vartheta_c})$ (cf. Assumption 2.4).*
 5. *The number of samples to compute the sample-averaged GNH is the same on all levels, i.e., $K_\ell = K$ independent of ℓ .*
 6. *For the single-level LIS constructed on level L , we assume that the LIS dimension satisfies $r_L^{\text{single}} \geq c r_0$ for some constant $c > 0$.*

The storage cost of the hierarchical LIS basis and the storage cost of the single-level LIS basis on level L are, respectively,

$$\zeta_{\text{multi}} = \sum_{\ell=0}^L R_\ell s_\ell, \quad \text{and} \quad \zeta_{\text{single}} = R_L r_L^{\text{single}}.$$

The floating point operations for one MVP with the hierarchical LIS basis and with the single-level LIS basis are $\mathcal{O}(\zeta_{\text{multi}})$ and $\mathcal{O}(\zeta_{\text{single}})$, respectively, with the same hidden constant.

COROLLARY 4.8. *The reduction factor of storing and operating with the hierarchical LIS basis (as opposed to the standard single-level LIS on level L) satisfies the upper bound*

$$(4.12) \quad \frac{\zeta_{\text{multi}}}{\zeta_{\text{single}}} \leq \frac{1}{c} \min \left(L + 1, \frac{1}{1 - e^{-|\beta_p - \beta_r|}} \right) e^{-\min(\beta_p, \beta_r)L}.$$

Proof. See Appendix A. □

Using a similar derivation, we can also obtain the reduction factor for constructing the hierarchical LIS basis. The number of MVPs (with the sample-averaged GNH $\widehat{\mathbf{H}}_0$) in the construction of the base level LIS via the eigenproblems (4.5) is linear in the number of leading eigenvectors obtained, i.e., $\mathcal{O}(s_0)$. The same holds for the number of MVPs with $\widehat{\mathbf{H}}_\ell$ in the construction of the auxiliary LIS vectors in the recursive enrichment solving the eigenproblems in (4.8). Thus, the overall computational complexities for constructing the hierarchical LIS basis is

$$\chi_{\text{multi}} = \mathcal{O} \left(K \sum_{\ell=0}^L s_\ell M_\ell^{\vartheta_c} \right).$$

Similarly, the construction of the single level LIS on level L is

$$\chi_{\text{single}} = \mathcal{O} \left(K r_L^{\text{single}} M_L^{\vartheta_c} \right),$$

where the prefactors are the same. The following corollary can be proved in the same way as Corollary 4.8, since we have assumed that $M_\ell^{\vartheta_c} = M_0^{\vartheta_c} e^{\beta_m \vartheta_c \ell}$.

COROLLARY 4.9. *The reduction factor of building the hierarchical LIS basis (as opposed to the standard single-level LIS basis on level L) satisfies the upper bound*

$$(4.13) \quad \frac{\chi_{\text{multi}}}{\chi_{\text{single}}} \leq \frac{1}{c} \min \left(L + 1, \frac{1}{1 - e^{-|\beta_m \vartheta_c - \beta_r|}} \right) e^{-\min(\beta_m \vartheta_c, \beta_r)L}.$$

5. Multilevel DILI. In this section, we first present a coupling strategy to construct positively correlated Markov chains for adjacent levels for computing multilevel MCMC estimators. The coupling strategy introduced in the original MLMCMC [13] can be viewed as a special case of our new approach. Utilising this coupling framework, we design a computationally efficient way to couple DILI proposals within MLMCMC by exploiting the structure of the hierarchical LIS.

5.1. Coupling strategy. We want to construct positively correlated Markov chains $\{\mathbf{V}_{\ell-1}^{(\ell,j)}\}$ and $\{\mathbf{V}_{\ell}^{(\ell,j)}\}$ for adjacent levels $\ell-1$ and ℓ with the invariant densities $\pi_{\ell-1}(\mathbf{v}_{\ell-1}|\mathbf{y})$ and $\pi_{\ell}(\mathbf{v}_{\ell}|\mathbf{y})$, respectively. As described in Section 3, this can be seen as sampling from the joint density $\Delta_{\ell,\ell-1}(\mathbf{v}_{\ell}, \mathbf{v}_{\ell-1})$ such that condition (3.2) holds and such that the within-level variance $\text{Var}_{\Delta_{\ell,\ell-1}}(D_{\ell})$ is reduced (cf. Remark 3.2).

Suppose the j -th states of the Markov chains at levels $\ell-1$ and ℓ are $\mathbf{V}_{\ell-1}^{(\ell,j)} = \mathbf{v}_{\ell-1}^*$ and $\mathbf{V}_{\ell}^{(\ell,j)} = \mathbf{v}_{\ell}^*$, respectively. The state at level ℓ has the form $\mathbf{v}_{\ell}^* = (\mathbf{v}_{\ell,c}^*, \mathbf{v}_{\ell,f}^*)$, corresponding to the coarse part of the parameters (shared with level $\ell-1$) and the refined part, respectively. We call the two Markov chains *coupled* at the j -th state if $\mathbf{v}_{\ell,c}^* = \mathbf{v}_{\ell-1}^*$. Assuming the two chains to be coupled at the j th state, the next states are proposed as follows.

PROPOSITION 5.1. *Given a set of posterior samples $\mathcal{V}_{\ell-1} = \{\mathbf{v}_{\ell-1}^{(i)}\}_{i=1}^{N_{\ell-1}}$ drawn from level $\ell-1$, we can define an empirical probability density in the form*

$$(5.1) \quad \tilde{\pi}_{\ell-1}(\mathbf{v}_{\ell-1}) = \frac{1}{N_{\ell-1}} \sum_{i=1}^{N_{\ell-1}} \delta(\mathbf{v}_{\ell-1} - \mathbf{v}_{\ell-1}^{(i)}).$$

Drawing a sample $\mathbf{v}'_{\ell-1}$ from the set $\mathcal{V}_{\ell-1}$ according to a uniform discrete distribution, the sample $\mathbf{v}'_{\ell-1}$ has the probability density

$$\tilde{\pi}_{\ell-1}(\mathbf{v}'_{\ell-1}) = \pi_{\ell-1}(\mathbf{v}'_{\ell-1}|\mathbf{y}).$$

It can be used as the proposal density for the coarse components in MH to sample from the fine chain $\{\mathbf{V}_{\ell}^{(\ell,j)}\}$, thus, positively correlating the two Markov chains.

The idea in Proposition 5.1 is discussed in [19, 37]. In the coupling strategy, we use the independent proposal defined by (5.1) to sample $\pi_{\ell-1}(\mathbf{v}_{\ell-1}|\mathbf{y})$. This way, the proposed candidate $\mathbf{v}'_{\ell-1} \sim \tilde{\pi}_{\ell-1}(\cdot)$ is independent of the current state $\mathbf{v}_{\ell-1}^*$. Given Proposition 5.1, the proposed state has acceptance probability one for sampling $\pi_{\ell-1}(\mathbf{v}_{\ell-1}|\mathbf{y})$. To sample $\pi_{\ell}(\mathbf{v}_{\ell}|\mathbf{y})$, we consider a factorised proposal in conditional form,

$$(5.2) \quad q(\mathbf{v}'_{\ell} | \mathbf{v}_{\ell}^*) = q(\mathbf{v}'_{\ell,c}, \mathbf{v}'_{\ell,f} | \mathbf{v}_{\ell}^*) = \tilde{\pi}_{\ell-1}(\mathbf{v}'_{\ell,c}) q(\mathbf{v}'_{\ell,f} | \mathbf{v}_{\ell}^*, \mathbf{v}'_{\ell,c}),$$

where the proposal candidate $\mathbf{v}'_{\ell,c}$ is set to be identical to the candidate $\mathbf{v}'_{\ell-1}$ from the previous level and where the proposal candidate \mathbf{v}'_{ℓ} conditioned on \mathbf{v}_{ℓ}^* can then be expressed as

$$(5.3) \quad \mathbf{v}'_{\ell,c} = \mathbf{v}'_{\ell-1} \quad (\text{copy from level } \ell-1 \text{ proposal}),$$

$$(5.4) \quad \mathbf{v}'_{\ell,f} \sim q(\cdot | \mathbf{v}_{\ell}^*, \mathbf{v}'_{\ell,c}) \quad (\text{conditional proposal}).$$

COROLLARY 5.2. *Using the factorised proposal (5.2) to sample from the level- ℓ posterior $\pi_{\ell}(\mathbf{v}_{\ell}|\mathbf{y})$, the acceptance probability takes the form*

$$(5.5) \quad \alpha_{\ell}^{\text{ML}}(\mathbf{v}_{\ell}^*, \mathbf{v}'_{\ell}) = \min \left\{ 1, \frac{\pi_{\ell}(\mathbf{v}'_{\ell}|\mathbf{y}) \pi_{\ell-1}(\mathbf{v}'_{\ell-1}|\mathbf{y}) q(\mathbf{v}_{\ell}^* | \mathbf{v}'_{\ell}, \mathbf{v}'_{\ell-1})}{\pi_{\ell}(\mathbf{v}_{\ell}^*|\mathbf{y}) \pi_{\ell-1}(\mathbf{v}_{\ell-1}^*|\mathbf{y}) q(\mathbf{v}'_{\ell}, \mathbf{v}'_{\ell-1} | \mathbf{v}_{\ell}^*)} \right\}.$$

Proof. The result follows directly from Proposition 5.1. \square

Figure 1 shows a schematic of the coupling strategy. The double dashed arrows represent the coupling of two MCMC states across the levels or the coupling of two proposal candidates across the levels. The dashed arrows represent the proposal and acceptance/rejection steps. The top half represents the Markov chain on level $\ell-1$, where all the proposed states are

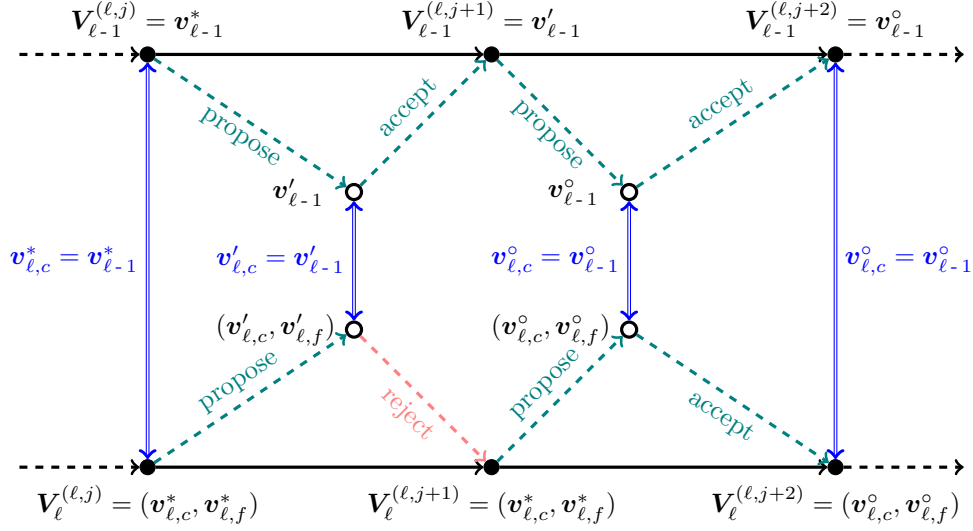


FIG. 1. A Diagram showing the coupling strategy.

accepted. The bottom half represents the Markov chain on level ℓ , where all the proposal candidates are coupled. All states on level ℓ that follow the acceptance of a proposal candidate are coupled with the corresponding states on level $\ell - 1$.

5.2. Coupled DILI proposal. The discretised DILI proposal (2.11) is

$$(5.6) \quad \mathbf{v}'_\ell = A_\ell \mathbf{v}_\ell^* + B_\ell \boldsymbol{\xi}_\ell, \quad \text{where } \boldsymbol{\xi}_\ell \sim \mathcal{N}(0, I_{R_\ell}),$$

as it was introduced in [10]. Suppose we have a LIS basis $\Psi_{\ell,r} \in \mathbb{R}^{R_\ell \times r_\ell}$. By treating the likelihood-informed parameter directions and the prior-dominated directions separately, we can construct the matrices A_ℓ and B_ℓ as

$$(5.7) \quad A_\ell = \Psi_{\ell,r} A_{\ell,r} \Psi_{\ell,r}^\top + a_\perp (I_{R_\ell} - \Pi_\ell) \in \mathbb{R}^{R_\ell \times R_\ell},$$

$$(5.8) \quad B_\ell^2 = \Psi_{\ell,r} B_{\ell,r}^2 \Psi_{\ell,r}^\top + b_\perp^2 (I_{R_\ell} - \Pi_\ell) \in \mathbb{R}^{R_\ell \times R_\ell},$$

where $A_{\ell,r}, B_{\ell,r} \in \mathbb{R}^{r_\ell \times r_\ell}$, a_\perp and $b_\perp \in \mathbb{R}$ and $\Pi_\ell = \Psi_{\ell,r} \Psi_{\ell,r}^\top$ are rank- r_ℓ orthogonal projectors.

COROLLARY 5.3. *In the proposal (5.6), suppose that $A_{\ell,r}, B_{\ell,r} \in \mathbb{R}^{r_\ell \times r_\ell}$ are non-singular matrices satisfying $A_{\ell,r}^2 + B_{\ell,r}^2 = I_{\ell,r}$, and a_\perp and b_\perp are scalars satisfying $a_\perp^2 + b_\perp^2 = 1$. Then, the corresponding proposal distribution $q(\mathbf{v}'_\ell | \mathbf{v}_\ell^*)$ satisfies the conditions of Theorem 2.3 and has the prior as its invariant measure, i.e., this proposal has acceptance probability one if we use it to sample the prior. The acceptance probability as samples from $\pi_\ell(\mathbf{v}_\ell | \mathbf{y})$ is*

$$(5.9) \quad \alpha(\mathbf{v}_\ell^*, \mathbf{v}'_\ell) = \min \left\{ 1, \exp \left[\eta_\ell(\mathbf{v}_\ell^*; \mathbf{y}) - \eta_\ell(\mathbf{v}'_\ell; \mathbf{y}) \right] \right\}.$$

Proof. Given $A_{\ell,r}^2 + B_{\ell,r}^2 = I_{\ell,r}$, the symmetric matrices $A_{\ell,r}$ and $B_{\ell,r}$ can be simultaneously diagonalised under some orthogonal transformation. Thus, the operators A_ℓ and B_ℓ can be simultaneously diagonalised, where the eigenspectrum of A_ℓ consists of the eigenvalues of $A_{\ell,r}$ and a_\perp , and the same applies to B_ℓ . This way, it is easy to check that the proposal distribution $q(\mathbf{v}'_\ell | \mathbf{v}_\ell^*)$ has the prior as invariant measure and that the conditions of Theorem 2.3 are satisfied. The form of the acceptance probability to sample from $\pi_\ell(\mathbf{v}_\ell | \mathbf{y})$ directly follows from the acceptance probability defined in Theorem 2.3. \square

We use the empirical posterior covariance, commonly used in adaptive MCMC [30, 16, 15] to construct matrices $A_{\ell,r}$ and $B_{\ell,r}$ for our DILI proposal (5.6). On each level, the empirical

covariance matrix $\Sigma_{\ell,r} \in \mathbb{R}^{r_\ell \times r_\ell}$ is estimated from past posterior samples projected onto the LIS. Given a jump size Δt , we can then define the matrices $A_{\ell,r}$ and $B_{\ell,r}^2$ by

$$\begin{aligned} A_{\ell,r} &= (2I_{r_\ell} + \Delta t \Sigma_{\ell,r})^{-1} (2I_{r_\ell} - \Delta t \Sigma_{\ell,r}) = I_{r_\ell} - 2(I_{r_\ell} + \frac{\Delta t}{2} \Sigma_{\ell,r})^{-1} (\frac{\Delta t}{2} \Sigma_{\ell,r}), \\ B_{\ell,r}^2 &= I_{r_\ell} - A_{\ell,r}^2 = 4(2I_{r_\ell} + (\frac{\Delta t}{2} \Sigma_{\ell,r})^{-1} + \frac{\Delta t}{2} \Sigma_{\ell,r})^{-1}, \end{aligned}$$

respectively. The operators $A_{\ell,r}$ and $B_{\ell,r}$ satisfy $A_{\ell,r}^2 + B_{\ell,r}^2 = I_{\ell,r}$ by construction.

5.2.1. Conditional DILI proposal. On level 0, the vanilla DILI proposal (cf. [10]) can be used to sample the Markov chain with invariant distribution $\pi_0(\mathbf{v}_0|\mathbf{y})$. On level ℓ , to simulate coupled Markov chains, the independent proposal $\tilde{\pi}_{\ell-1}(\mathbf{v}_{\ell-1})$, as defined in (5.1), is used to sample the posterior $\pi_{\ell-1}(\mathbf{v}_{\ell-1}|\mathbf{y})$, while the factorised proposal

$$q(\mathbf{v}'_\ell | \mathbf{v}^*_\ell) = \tilde{\pi}_{\ell-1}(\mathbf{v}'_{\ell,c}) q(\mathbf{v}'_{\ell,f} | \mathbf{v}^*_\ell, \mathbf{v}'_{\ell,c}),$$

is used to sample $\pi_\ell(\mathbf{v}_\ell|\mathbf{y})$. We now use DILI to generate the fine components $\mathbf{v}'_{\ell,f}$ of the proposal candidate and thus to fix the conditional probability $q(\mathbf{v}'_{\ell,f} | \mathbf{v}^*_\ell, \mathbf{v}'_{\ell,c})$. Defining the precision matrix

$$(5.10) \quad P_\ell = B_\ell^{-2} = \Psi_{\ell,r} B_{\ell,r}^{-2} \Psi_{\ell,r}^\top + b_\perp^{-2} (I_{R_\ell} - \Pi_\ell),$$

the DILI proposal (5.6) can be split as follows:

$$(5.11) \quad \begin{bmatrix} \mathbf{v}'_{\ell,c} \\ \mathbf{v}'_{\ell,f} \end{bmatrix} = A_\ell \mathbf{v}^*_\ell + \begin{bmatrix} \mathbf{r}_{\ell,c} \\ \mathbf{r}_{\ell,f} \end{bmatrix}, \quad \begin{bmatrix} \mathbf{r}_{\ell,c} \\ \mathbf{r}_{\ell,f} \end{bmatrix} \sim \mathcal{N}\left(0, \begin{bmatrix} P_{\ell,cc} & P_{\ell,cf} \\ P_{\ell,fc} & P_{\ell,ff} \end{bmatrix}^{-1}\right),$$

where the partitions of the vectors and of the matrix P_ℓ correspond to the parameter coordinates shared with level $\ell-1$ and the refined parameter coordinates on level ℓ .

DEFINITION 5.4. *The following procedure is used to draw candidates from the factorised proposal distribution $\tilde{\pi}_{\ell-1}(\mathbf{v}'_{\ell,c}) q(\mathbf{v}'_{\ell,f} | \mathbf{v}^*_\ell, \mathbf{v}'_{\ell,c})$ such that the DILI proposal in (5.11) is used as the conditional distribution $q(\mathbf{v}'_{\ell,f} | \mathbf{v}^*_\ell, \mathbf{v}'_{\ell,c})$:*

1. *The proposed candidate $\mathbf{v}'_{\ell,c}$ is randomly selected from the sample set $\mathcal{V}_{\ell-1}$, as defined in Proposition 5.1. Note that the sample $\mathbf{v}'_{\ell,c}$ is identical to the proposal candidate $\mathbf{v}'_{\ell-1}$ used for sampling $\pi_{\ell-1}(\mathbf{v}_{\ell-1}|\mathbf{y})$, c.f. (5.3).*
2. *Since $\mathbf{v}'_{\ell,c}$ and \mathbf{v}^*_ℓ are known, the variable $\mathbf{r}_{\ell,c}$ can be determined from (5.11) as*

$$\mathbf{r}_{\ell,c} = \mathbf{v}'_{\ell,c} - \Theta_{\ell,c}^\top A_\ell \mathbf{v}^*_\ell.$$

3. *Then, we can draw a random variable $\mathbf{r}_{\ell,f}$ conditioned on $\mathbf{r}_{\ell,c}$ such that the joint distribution of $(\mathbf{r}_{\ell,c}, \mathbf{r}_{\ell,f})$ follows the Gaussian $\mathcal{N}(0, P_\ell^{-1})$. Due to (5.11), the refined part of the proposed candidate $\mathbf{v}'_{\ell,f}$ satisfies*

$$(5.12) \quad \mathbf{v}'_{\ell,f} = \Theta_{\ell,f}^\top A_\ell \mathbf{v}^*_\ell + \mathbf{r}_{\ell,f}, \quad \mathbf{r}_{\ell,f} \sim \mathcal{N}(-P_{\ell,ff}^{-1} P_{\ell,fc} \mathbf{r}_{\ell,c}, P_{\ell,ff}^{-1}),$$

where $\mathbf{r}_{\ell,f}$ is a conditional Gaussian random vector.

COROLLARY 5.5. *Using the above procedure to draw candidates from the factorised proposal distribution $\tilde{\pi}_{\ell-1}(\mathbf{v}'_{\ell,c}) q(\mathbf{v}'_{\ell,f} | \mathbf{v}^*_\ell, \mathbf{v}'_{\ell,c})$, the acceptance probability to sample from the posterior distribution $\pi_\ell(\mathbf{v}_\ell|\mathbf{y})$ is*

$$\alpha_\ell^{\text{ML}}(\mathbf{v}^*_\ell, \mathbf{v}'_\ell) = \min \left\{ 1, \exp \left[\left(\eta_\ell(\mathbf{v}^*_\ell; \mathbf{y}) - \eta_{\ell-1}(\mathbf{v}^*_{\ell-1}; \mathbf{y}) \right) - \left(\eta_\ell(\mathbf{v}'_\ell; \mathbf{y}) - \eta_{\ell-1}(\mathbf{v}'_{\ell-1}; \mathbf{y}) \right) \right] \right\}.$$

Proof. See Appendix B. □

5.2.2. Generating conditional samples. The computational cost of the coupling procedure is dictated by the multiplication with A_ℓ in Step 2 and the generation of conditional proposal samples in Step 3. The multiplication with A_ℓ has a computational complexity of $\mathcal{O}(\sum_{j=0}^{\ell} R_j s_j)$ using the low-rank representation (5.7) and the upper-triangular hierarchical

LIS basis in (4.11), which has the form

$$\Psi_{\ell,r} = [\Psi_{\ell,c}, \Psi_{\ell,f}] = \begin{bmatrix} \Psi_{\ell-1,r} & Z_{\ell,c} \\ 0 & Z_{\ell,f} \end{bmatrix}.$$

We can also exploit the hierarchical LIS to reduce the computational cost of generating conditional proposal samples. As shown in Equation (5.10), given the LIS basis $\Psi_{\ell,r}$, the precision matrix P_ℓ is dictated by the matrix $B_{\ell,r}^{-2}$, which has the block form

$$(5.13) \quad B_{\ell,r}^{-2} = \begin{bmatrix} \Xi_{\ell,cc} & \Xi_{\ell,cf} \\ \Xi_{\ell,fc} & \Xi_{\ell,ff} \end{bmatrix},$$

corresponding to the splitting of the enriched LIS basis into $\Psi_{\ell,c}$ and $\Psi_{\ell,f}$. Generating conditional proposal samples only involves the blocks $P_{\ell,ff}$ and $P_{\ell,fc}$ in the matrix P_ℓ , i.e.,

$$(5.14) \quad P_{\ell,ff} = Z_{\ell,f} (\Xi_{\ell,ff} - b_\perp^{-2} \mathbf{I}) Z_{\ell,f}^\top + b_\perp^{-2} \mathbf{I}_{\ell,f},$$

$$(5.15) \quad P_{\ell,fc} = Z_{\ell,f} \Xi_{\ell,fc} \Psi_{\ell-1,r}^\top + Z_{\ell,f} \Xi_{\ell,ff} Z_{\ell,c}^\top - b_\perp^{-2} Z_{\ell,f} Z_{\ell,c}^\top,$$

which in turn only require the blocks $\Xi_{\ell,fc} \in \mathbb{R}^{s_\ell \times r_{\ell-1}}$ and $\Xi_{\ell,ff} \in \mathbb{R}^{s_\ell \times s_\ell}$ in the matrix $B_{\ell,r}^{-2}$.

We derive low-rank operations to avoid the direct inversion or factorisation of the matrices $P_{\ell,ff}$ and $P_{\ell,fc}$ in the generation of conditional samples and to reduce the computational cost. Suppose the block $Z_{\ell,f} \in \mathbb{R}^{(R_\ell - R_{\ell-1}) \times s_\ell}$ has the thin QR factorisation

$$(5.16) \quad Z_{\ell,f} = U_\ell T_\ell,$$

where U_ℓ has orthonormal columns and T_ℓ is upper triangular. Then the matrix $P_{\ell,ff}$ can be expressed as

$$P_{\ell,ff} = b_\perp^{-2} \left(U_\ell (T_\ell (b_\perp^2 \Xi_{\ell,ff} - \mathbf{I}) T_\ell^\top) U_\ell^\top + \mathbf{I}_{\ell,f} \right).$$

Computing the $s_\ell \times s_\ell$ eigendecomposition

$$(5.17) \quad T_\ell (b_\perp^2 \Xi_{\ell,ff} - \mathbf{I}) T_\ell^\top = W_\ell D_\ell W_\ell^\top,$$

where W_ℓ and D_ℓ are respectively orthogonal and diagonal matrices, we have

$$P_{\ell,ff} = b_\perp^{-2} \left(\Phi_\ell D_\ell \Phi_\ell^\top + \mathbf{I}_{\ell,f} \right), \quad \text{with } \Phi_\ell := U_\ell W_\ell.$$

Note that $\Phi_\ell \in \mathbb{R}^{(R_\ell - R_{\ell-1}) \times s_\ell}$ has orthonormal columns, so that

$$(5.18) \quad P_{\ell,ff}^{-1} P_{\ell,fc} = b_\perp^2 \underbrace{\Phi_\ell ((D_\ell + \mathbf{I})^{-1} W_\ell^\top T_\ell)}_{s_\ell \times s_\ell} \underbrace{(\Xi_{\ell,fc} \Psi_{\ell-1,r}^\top + \Xi_{\ell,ff} Z_{\ell,c}^\top - b_\perp^{-2} Z_{\ell,c}^\top)}_{s_\ell \times R_{\ell-1}},$$

$$(5.19) \quad P_{\ell,ff}^{-\frac{1}{2}} = b_\perp \left(\underbrace{\Phi_\ell ((D_\ell + \mathbf{I})^{-\frac{1}{2}} - \mathbf{I})}_{s_\ell \times s_\ell} \Phi_\ell^\top + \mathbf{I}_{\ell,f} \right).$$

Using these representations of the matrices $P_{\ell,ff}^{-1} P_{\ell,fc}$ and $P_{\ell,ff}^{-1/2}$, the conditional Gaussian in (5.12) can be simulated efficiently using

$$(5.20) \quad \mathbf{r}_{\ell,f} | \mathbf{r}_{\ell,c} = -P_{\ell,ff}^{-1} P_{\ell,fc} \mathbf{r}_{\ell,c} + P_{\ell,ff}^{-\frac{1}{2}} \xi, \quad \text{where } \xi \sim \mathcal{N}(0, \mathbf{I}_{(R_\ell - R_{\ell-1})}).$$

The associated computational cost is $\mathcal{O}(R_\ell s_\ell)$.

5.3. Final MLDILI algorithm. Here, we assemble all the elements of the multilevel DILI method defined in previous sections in algorithmic form. For the base level ($\ell = 0$), the LIS construction and the DILI-MCMC sampling are presented in Algorithm 5.1. The recursive LIS construction and the coupled DILI-MCMC are presented in Algorithm 5.2.

In both algorithms, we need to use both the LIS basis $\Psi_{\ell,r}$ and an empirical covariance matrix $\Sigma_{\ell,r}$ projected onto the LIS to define operators A_ℓ and B_ℓ in the DILI proposal. Computing the LIS basis needs some reference distribution $p_\ell^*(\cdot)$. We employ the Laplace approximation

Algorithm 5.1 Base level algorithm.

Input: A set of samples $\mathcal{W}_0 = \{\mathbf{v}_0^{(k)}\}_{k=1}^{K_0}$ drawn from the base level reference $p_0^*(\cdot)$, the number of MCMC iterations N_0 , and an initial MCMC state $\mathbf{V}_0^{(0)}$.

Output: A LIS basis $\Psi_{0,r}$ and a Markov chain of posterior samples $\mathcal{V}_0 = \{\mathbf{V}_0^{(j)}\}_{j=1}^{N_0}$.

- 1: **procedure** BASE LEVEL LIS AND MCMC
- 2: Use \mathcal{W}_0 to solve the eigenproblem in (4.5) to obtain the base level LIS basis $\Psi_{0,r}$.
- 3: Estimate the empirical covariance matrix $\Sigma_{0,r}$ from the samples in \mathcal{W}_0 and define the operators A_0 and B_0 as in (5.7)–(5.8).
- 4: **for** $j = 1, \dots, N_0$ **do**
- 5: Propose a candidate \mathbf{v}'_0 using the base level proposal in (5.6).
- 6: Compute the acceptance probability $\alpha(\mathbf{V}_0^{(j-1)}, \mathbf{v}'_0)$ defined in (5.9).
- 7: With probability $\alpha(\mathbf{V}_0^{(j-1)}, \mathbf{v}'_0)$, set $\mathbf{V}_0^{(j)} = \mathbf{v}'_0$, otherwise set $\mathbf{V}_0^{(j)} = \mathbf{V}_0^{(j-1)}$.
- 8: **end for**
- 9: **end procedure**

Note: Optionally, $\Sigma_{0,r}$, A_0 and B_0 can be adaptively updated within the MCMC after a pre-fixed number of iterations, cf. [1, 16].

Algorithm 5.2 Level- ℓ algorithm.

Input: A set of samples $\mathcal{W}_\ell = \{\mathbf{v}_\ell^{(k)}\}_{k=1}^{K_\ell}$ from the level- ℓ reference $p_\ell^*(\cdot)$, the number of MCMC iterations N_ℓ , a set of MCMC samples $\mathcal{V}_{\ell-1} = \{\mathbf{v}_{\ell-1}^{(j)}\}_{j=1}^{N_{\ell-1}}$ on level $\ell-1$ and an initial MCMC state $\mathbf{V}_\ell^{(0)}$.

Output: A LIS basis $\Psi_{\ell,r}$ and a Markov chain of posterior samples $\mathcal{V}_\ell = \{\mathbf{V}_\ell^{(j)}\}_{j=1}^{N_\ell}$.

- 1: **procedure** LEVEL- ℓ LIS AND MCMC
- 2: Lift previous LIS basis, $\Psi_{\ell,c} = \Theta_{\ell,c} \Psi_{\ell-1,r}$.
- 3: Use \mathcal{W}_ℓ to solve the eigenproblem in (4.8) to obtain the auxiliary LIS vectors $\Psi_{\ell,f}$.
- 4: Estimate the empirical covariance matrix $\Sigma_{\ell,r}$ from the samples in \mathcal{W}_ℓ and define the operators A_ℓ and B_ℓ as in (5.7)–(5.8).
- 5: Compute the matrices $P_{\ell,ff}^{-1} P_{\ell,fc}$ and $P_{\ell,ff}^{-\frac{1}{2}}$ as in (5.18)–(5.19).
- 6: **for** $j = 1, \dots, N_\ell$ **do**
- 7: Propose a candidate $\mathbf{v}'_\ell = (\mathbf{v}'_{\ell,c}, \mathbf{v}'_{\ell,f})$ using Definition 5.4, which needs $\mathcal{V}_{\ell-1}$.
- 8: Compute the acceptance probability $\alpha_\ell^{\text{ML}}(\mathbf{V}_\ell^{(j-1)}, \mathbf{v}'_\ell)$ defined in Corollary 5.5.
- 9: With probability $\alpha_\ell^{\text{ML}}(\mathbf{V}_\ell^{(j-1)}, \mathbf{v}'_\ell)$, set $\mathbf{V}_\ell^{(j)} = \mathbf{v}'_\ell$, otherwise set $\mathbf{V}_\ell^{(j)} = \mathbf{V}_\ell^{(j-1)}$.
- 10: **end for**
- 11: **end procedure**

Note: Optionally, $\Sigma_{\ell,r}$, A_ℓ , B_ℓ , and the matrices $P_{\ell,ff}^{-1} P_{\ell,fc}$ and $P_{\ell,ff}^{-\frac{1}{2}}$ can be adaptively updated within MCMC after a pre-fixed number of iterations.

to the posterior (e.g., [27, 29]). This way, all the samples from $p_\ell^*(\cdot)$ can be generated in parallel and prior to the DILI-MCMC simulation. The empirical covariance $\Sigma_{\ell,r}$ can be estimated using either samples drawn from the reference distribution (before the start of MCMC) or adaptively using posterior samples generated in MCMC. The latter option is the classical adaptive MCMC method [16]. The adaptation of $\Sigma_{\ell,r}$ is optional in Algorithms 5.1 and 5.2. Similar to the adaptation of the covariance, the LIS basis can also be adaptively updated using newly generated posterior samples during MCMC simulations. The implementation details for the adaptation of the LIS can be found in Algorithm 1 of [10].

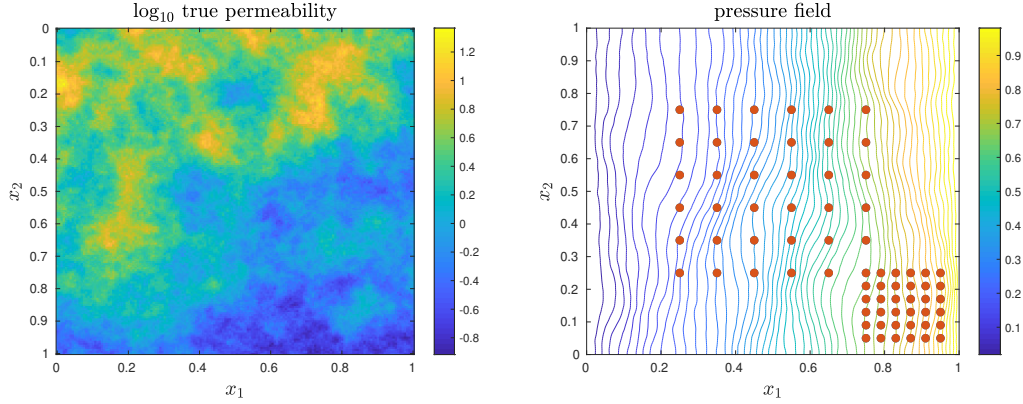


FIG. 2. Setup of elliptic inverse problem. Left: “true” permeability field used for generating the synthetic data set. Right: observation sensors (red dots) and pressure field corresponding to “true” permeability field.

6. Numerical experiments. In this section, we test our algorithms on test problem involving an elliptic PDE with random coefficients. The setup is described in section 6.1, while numerical comparisons are given in section 6.2.

6.1. Setup. We consider an elliptic PDE in a domain $\Omega = [0, 1]^2$ with boundary $\partial\Omega$, which models, e.g., the pressure distribution $p(\mathbf{x})$ of a stationary fluid in a porous medium described by a spatially heterogeneous permeability field $k(\mathbf{x})$. Here, $\mathbf{x} \in \Omega$ denotes the spatial coordinate and $\mathbf{n}(\mathbf{x})$ denotes the outward normal vector along the boundary.

The goal is to recover the permeability field from pressure observations. We assume that the permeability field follows a log-normal prior, and thus we denote the permeability field by $k(\mathbf{x}) = \exp(u(\mathbf{x}))$, where $u(\mathbf{x})$ is a random function equipped with a Gaussian process prior. In this setting, the pressure $p(\mathbf{x})$ depends implicitly on the (random) realisation of $u(\mathbf{x})$.

For a given realisation $u(\mathbf{x})$, the pressure satisfies the elliptic PDE

$$(6.1) \quad -\nabla \cdot (e^{u(\mathbf{x})} \nabla p(\mathbf{x})) = 0, \quad \mathbf{x} \in \Omega.$$

On the left and right boundaries, we specify Dirichlet boundary conditions, while on the top and bottom we assume homogeneous Neumann boundary conditions:

$$(6.2) \quad \begin{cases} p(\mathbf{x}) = 0, & \text{for } \mathbf{x} \in \partial\Omega_{\text{left}}, \\ p(\mathbf{x}) = 1, & \text{for } \mathbf{x} \in \partial\Omega_{\text{right}} \text{ and} \\ e^{u(\mathbf{x})} \nabla p(\mathbf{x}) \cdot \mathbf{n}(\mathbf{x}) = 0, & \text{for } \mathbf{x} \in \{\partial\Omega_{\text{top}}, \partial\Omega_{\text{bottom}}\}. \end{cases}$$

As the quantity of interest, we define the outflow through the left vertical boundary, i.e.

$$(6.3) \quad Q(u) = -\int_0^1 e^{u(\mathbf{x})} \frac{\partial p(\mathbf{x})}{\partial x_1} \Big|_{x_1=0} dx_2 = -\int_{\Omega} e^{u(\mathbf{x})} \nabla p(\mathbf{x}) \cdot \nabla \varphi(\mathbf{x}) d\mathbf{x},$$

where $\varphi(\mathbf{x})$ is a linear function taking value one on $\partial\Omega_{\text{left}}$ and value zero on $\partial\Omega_{\text{right}}$, as suggested in [36].

The Gaussian process prior for $u(\mathbf{x})$ is defined by the exponential kernel $k(\mathbf{x}, \mathbf{x}') = \exp(-5|\mathbf{x} - \mathbf{x}'|)$. Figure 2 (left) displays the true (synthetic) permeability field in \log_{10} scale. Noisy observations of the pressure field are collected from 71 sensors located as in Figure 2 (right), with a signal-to-noise ratio 50. A likelihood function can then be defined as in (2.3), which, together with the prior, characterizes the posterior distribution in (2.1).

In practice, (6.1)–(6.3) has to be solved numerically. We use standard, piecewise bilinear finite elements on a hierarchy of nested Cartesian grids with mesh size $h_{\ell} = \frac{1}{20} \times 2^{-\ell}$, for $\ell =$

Level	0	1	2	3
Non-recursive	80	91	97	100
Recursive (added on level ℓ)	80	21	19	12
Recursive (total)	80	101	120	132
Storage reduction factor	1	0.74	0.60	0.43

TABLE 1

LIS dimensions: Results of non-recursive construction (single-level LIS for each ℓ) reported in first row; for the recursive construction, the number of vectors added on the current level and the total LIS dimension are given in the second and third row, respectively; the fourth row displays the storage reduction factor for the recursive procedure at each level.

Level	Refined parameters		D_ℓ	
	MLDILI	MLpCN	MLDILI	MLpCN
0	34	4300	9.0	4100
1	11	45	4.6	4.9
2	3.6	48	2.4	2.8
3	2.0	24	1.8	1.9

TABLE 2

Comparison of IACTs of Markov chains generated by MLDILI and MLpCN. This table reports the IACTs of the refined parameters and the level- ℓ correction of the quantity of interest $D_\ell = Q_\ell(\mathbf{V}_\ell) - Q_{\ell-1}(\mathbf{V}_{\ell-1})$.

0, 1, 2, 3. Furthermore, we approximate the unknown function $u(\mathbf{x})$ by truncated Karhunen-Loève expansions with $R_\ell = 50 + 100 \times 2^\ell$ random modes, respectively.

6.2. Comparisons. In this section, we test and compare our algorithms on the model problem described above. First, we proceed as in section 4 to build a LIS at every level, both with the non-recursive and recursive constructions. Table 1 summarizes the number of basis functions obtained in each case using the truncation threshold $\rho = 10^{-2}$ and the storage reduction factor given by the recursive procedure at each level.

Because the recursive LIS construction recycles LIS bases from previous levels and enriches them with a number of auxiliary LIS vectors on each level, it is expected that the total number of basis functions obtained by the enriching procedure at each level is slightly higher than the direct (spectral) LIS on the same level. However, in the recursive construction, the dimension of the auxiliary set of vectors is expected to decrease as the level increases, requiring less storage and less computational effort on the finer levels, since the posterior distributions were assumed to converge with $\ell \rightarrow \infty$. For problems with parametrisations where the parameter dimension increases more rapidly with the discretisation level—e.g., using the same finite element grid to discretise the prior covariance, the setting used in the original DILI paper [10]—we expect the reduction factor to be even smaller.

In the comparison of sampling performances, we denote by **MLpCN** the MLMCMC algorithm using the pCN proposal for the additional parameters on each level (as in [13]), but using the coupling procedure in Proposition 5.1. The MLMCMC algorithm using the recursive LIS and the coupled DILI proposals, as summarised in Algorithms 5.1 and 5.2, is denoted by **MLDILI**. The integrated autocorrelation times of Markov chains constructed by MLpCN and MLDILI are reported in Table 2. The IACTs for two functionals are reported for each algorithm. In the “refined parameters” case, at every level ℓ we report the average IACTs of the refined parameters $\mathbf{v}_{\ell,f}$. This quantifies how well the algorithm performs in exploring the posterior distribution. In the second case, we consider the IACT of the level- ℓ corrections of the quantity of interest $D_\ell = Q_\ell(\mathbf{V}_\ell) - Q_{\ell-1}(\mathbf{V}_{\ell-1})$.

In the “refined parameters” case, we observe a significant improvement for MLDILI over

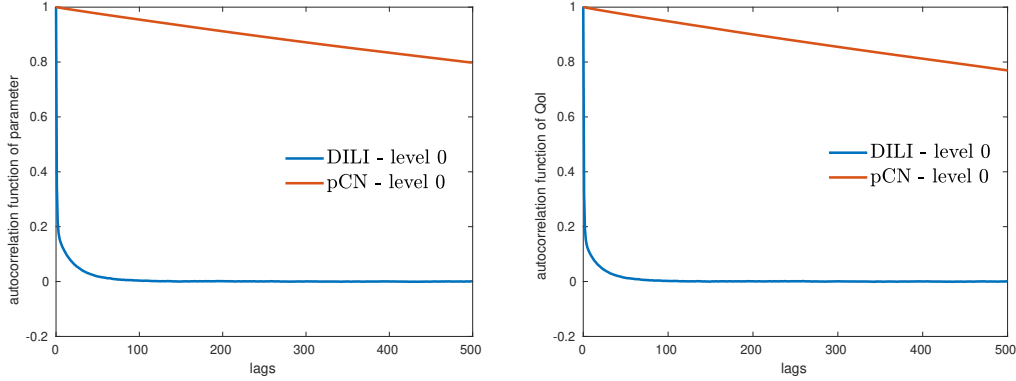


FIG. 3. IACTs of the chains $\{(\mathbf{V}_0^{(j)})_1\}$ and $\{Q_0(\mathbf{V}_0^{(j)})\}$ on the coarsest level (Blue: DILI. Red: pCN).

MLpCN: the coupled DILI proposal is able to reduce the IACT at every level compared to that obtained by MLpCN. At the base level, DILI is able to reduce the IACT by two orders of magnitude compared to that of pCN. This suggests that coarse parameter modes are very informed by the data, and thus utilising the DILI proposal is highly beneficial. In the case of the quantity of interest, we observe an even more impressive improvement at the base level (a factor of 456!), while the IACTs of MLDILI and MLpCN on the finer levels are comparable. This suggests that the posterior distribution of the chosen quantity of interest (the integrated flux over the boundary) is not affected strongly by the high frequency parameter modes on the finer levels. Nevertheless, in both cases, using DILI provides a huge acceleration compared to pCN. Figure 3 compares the integrated autocorrelation times of DILI and pCN on level 0, for both the first parameter component and the quantity of interest.

The IACTs for the level- ℓ corrections of the quantity of interest in Table 2 suggest that using a mixed strategy—in which one employs the LIS and DILI only at the coarsest level and uses pCN in refined levels—is also a reasonable approach in cases where the important likelihood-informed directions that have any influence on the quantity of interest are already well enough identified in the base-level LIS. We refer to this as the **MLmixed** strategy.

We compare the computational performance of the three multilevel algorithms (MLDILI, MLpCN, MLmixed) with the two single level algorithms using DILI and pCN proposals. The finite element model and all MCMC algorithms are implemented in MATLAB; we use sparse Cholesky factorisation [6] to solve the finite element systems and ARPACK [26] to solve the eigenproblems. All simulations are carried out on a workstation equipped with 28 cores (two Intel Xeon E5-2680 CPUs). The performance of MLmixed is only estimated using the IACTs and the actual computing times measured in the MLDILI and MLpCN runs.

The computational complexities of the five algorithms for approximating $\mathbb{E}_\pi[Q]$ on (discretisation) levels $L = 1, 2$ and 3 with Q defined in (6.3) are compared in Figure 4 (right). In the multilevel estimators, the coarsest level is always $\ell = 0$, so that the number of levels is 2, 3 and 4, respectively. The sampling error tolerance on each level is adapted to the corresponding bias error due to finite element discretisation and parameter truncation, such that the squared bias is equal to the variance of the estimator. The bias errors were estimated beforehand to be 9×10^{-3} , 4×10^{-3} , and 2×10^{-3} on levels $L = 1, 2$ and 3, leading to a total error of 1.27×10^{-2} , 5.7×10^{-3} , 2.8×10^{-3} , respectively. Those bias estimates are plotted in Figure 4 (left) together with estimates of $\text{Var}_{\pi_\ell}(Q_\ell)$ and $\text{Var}_{\Delta_{\ell,\ell-1}}(Q_\ell - Q_{\ell-1})$, which suggest that $\theta_b \approx 0.5$ and $\theta_v \approx 0.5$ in Assumptions 2.4(i) and 3.3. This agrees with the theoretical results in [13]. The cost per sample is dominated by the sparse Cholesky factorisation on each level and scales roughly like $\mathcal{O}(M_\ell^{1.2})$, so that $\theta_c \approx 1.2$ in Assumption 2.4(ii). Optimally scaling

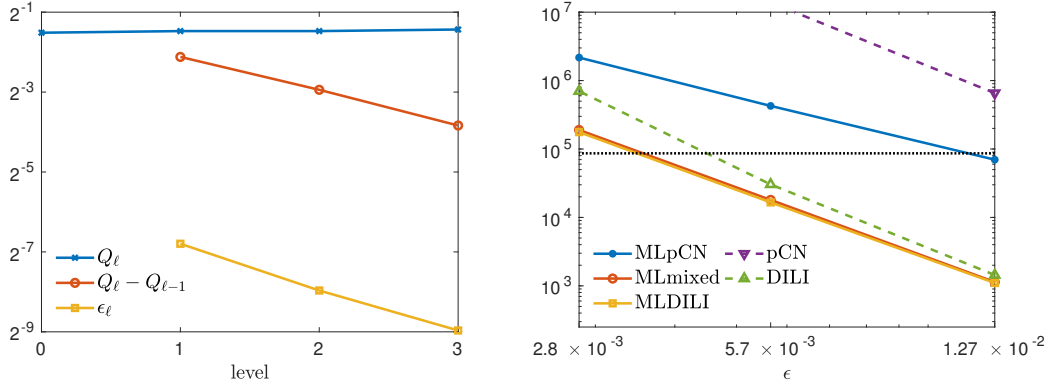


FIG. 4. Left: the variance $\text{Var}_{\pi_\ell}(Q_\ell)$ (blue) and the bias $|\mathbb{E}_{\mu_y}[Q] - \mathbb{E}_{\pi_\ell}[Q_\ell]|$ (yellow) at each level, and the cross-level variances $\text{Var}_{\Delta_{\ell,\ell-1}}(Q_\ell - Q_{\ell-1})$ (red) used for estimating the CPU time for various MCMC methods. Right: Total CPU time (in seconds) for various methods to achieve different total error tolerances. The LISs are constructed by recycling Cholesky factors. The dotted line represents a CPU day.

multigrid solvers exist for this model problem, but for the FE problem sizes considered here they are more costly in absolute terms. Moreover, we can also exploit the fact that the adjoint problem is identical to the forward problem here, so that the Cholesky factors can be reused for the adjoint solves required in the LIS construction.

Let us now discuss the results. The single level pCN becomes impractical in this example, since the data is very informative and leads to an extremely low effective sample size. Some of this bad statistical efficiency is inherited by MLpCN, at least in absolute terms, due to the poor effective sample size on level 0. Asymptotically this effect disappears and the rate of growth of the cost is smallest for MLpCN with an observed asymptotic cost of about $\mathcal{O}(\epsilon^{-2.3})$. As observed in [13], this is better than the theoretically predicted asymptotic rate and is likely a pre-asymptotic effect due to the high cost on level 0. Unsurprisingly, given the low IACTs reported in Table 2, the methods based on DILI proposals all perform significantly better. MLDILI and MLmixed perform almost identically, since the corresponding IACTs on all levels are very similar. They are consistently better than single-level DILI and the asymptotic rate of growth of the cost is also better, $\mathcal{O}(\epsilon^{-3.4})$ compared to $\mathcal{O}(\epsilon^{-4.1})$. Both rates are consistent with the theoretically predicted rates in Theorem 3.5, given the estimates for $\theta_b, \theta_v, \theta_c$ above. For the most accurate estimates, MLDILI is almost 4 times faster than DILI, and due to the better asymptotic behaviour this reduction factor will grow as $\epsilon \rightarrow 0$. For grid level $L = 4$, we even expect MLpCN to outperform single-level DILI, but the computational costs of the estimators for higher accuracies are starting to become impractical even using the multilevel acceleration, as the dashed line representing one CPU day in Figure 4 (right) indicates.

The dominating cost in solving the eigenproblems (4.5) and (4.8) is the Cholesky factorisation. As mentioned above, sparse direct solvers are used to solve the stationary forward model and we are able to recycle the Cholesky factors from the forward solve to compute the actions of the adjoint model in (4.5) and (4.8) for each sample. As a result, the computational cost of building the LIS is negligible compared to that of the MCMC simulation here (for both the single level and the recursive construction). This also explains why MLmixed performs almost identically to MLDILI.

However, in many other applications this is not possible due to the high storage cost or when the adjoint is different. Each action of the adjoint problem typically has a comparable cost to solving the forward model in the stationary case. It can even be more expensive than solving the forward model in time-dependent problems. To provide a thorough comparison in that case, we also report the total CPU time of all the estimators in Figure 5 when the

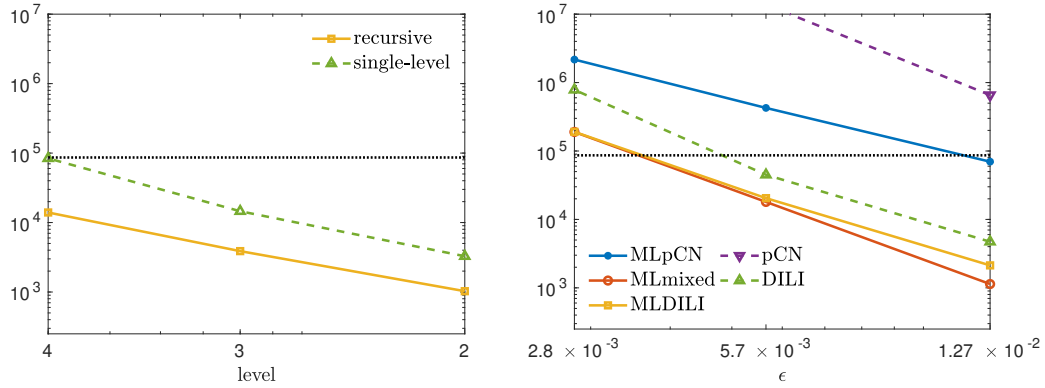


FIG. 5. *Left: Total CPU time (in seconds) for the single level and recursive constructions of the LISs at level 2, 3 and 4. Right: Total CPU time (in seconds) for various methods to achieve different error tolerances. The LISs are constructed without recycling Cholesky factors. The dotted line represents a CPU day.*

LIS setup cost is included. Here, we compute both the single level LIS and the recursive LIS without storing the Cholesky factors, to mimic the behaviour in the general, large-scale case. In this setup, we observe that a significant amount of computing effort is spent on building the LIS, and thus MLmixed and MLDILI significantly outperform the single level DILI for all error thresholds. MLmixed is more than 4 times faster than DILI even for the largest error threshold of 1.27×10^{-2} . The construction of the single-level LIS requires two times more CPU time than performing the actual MCMC simulation in that case. In comparison, a significant number of adjoint model solves can be saved by the recursive LIS construction. Furthermore, we do expect that the computational cost for constructing the recursive LIS will stop increasing, since the dimension of the auxiliary LIS will eventually be zero at higher levels. Overall, for large-scale problems where the adjoint cannot be cheaply computed by recycling the forward model simulation, the recursive LIS construction, and hence the MLDILI, is clearly more computationally efficient than the single level DILI.

7. Conclusion. We integrate the dimension-independent likelihood-informed MCMC from [10] into the multilevel MCMC framework in [13] to improve the computational efficiency of estimating the expectation of functionals of interests over posterior measures. Several novel elements are introduced in this integration. We first design a Rayleigh-Ritz procedure to recursively construct likelihood informed subspaces that exploit the hierarchy of model discretisations. The resulting hierarchical LIS needs lower computational effort to construct and has lower operation cost compared to the original LIS proposed in [11]. Then, we present a new pooling strategy to couple Markov chains on consecutive levels. This enables more flexible parallelisation and management of computing resources. Finally, we design new coupled DILI proposals by exploiting the hierarchical LIS, so that the DILI proposal can be applied in the multilevel MCMC setting. We also demonstrate the efficacy of our integrated approach on a model inverse problem governed by an elliptic PDE.

Appendix A. Proof of Corollary 4.8. Using Assumption 4.7, the required storage for the hierarchical and for the single-level LIS bases can be bounded by

$$\zeta_{\text{multi}} = \sum_{\ell=0}^L R_{\ell} s_{\ell} \leq R_0 s_0 \sum_{\ell=0}^L e^{(\beta_p - \beta_r)\ell} \quad \text{and} \quad \zeta_{\text{single}} = R_L r_L \geq c R_0 s_0 e^{\beta_p L}.$$

Thus, the reduction factor satisfies

$$(A.1) \quad \frac{\zeta_{\text{multi}}}{\zeta_{\text{single}}} \leq \frac{1}{c} e^{-\beta_p L} \left(\sum_{\ell=0}^L e^{(\beta_p - \beta_r)\ell} \right).$$

We first consider the case $\beta_p \neq \beta_r$. Using the property of geometric series, we have

$$\sum_{\ell=0}^L e^{(\beta_p - \beta_r)\ell} = \frac{1 - e^{(\beta_p - \beta_r)(L+1)}}{1 - e^{(\beta_p - \beta_r)}}.$$

For the case $\beta_p < \beta_r$, the reduction factor satisfies

$$(A.2) \quad \frac{\zeta_{\text{multi}}}{\zeta_{\text{single}}} \leq \frac{1}{c} e^{-\beta_p L} \frac{1 - e^{(\beta_p - \beta_r)(L+1)}}{1 - e^{(\beta_p - \beta_r)}},$$

whereas for $\beta_p > \beta_r$, the reduction factor satisfies

$$(A.3) \quad \frac{\zeta_{\text{multi}}}{\zeta_{\text{single}}} \leq \frac{1}{c} e^{-\beta_p L} \frac{1 - e^{(\beta_p - \beta_r)(L+1)}}{1 - e^{(\beta_p - \beta_r)}} = \frac{1}{c} e^{-\beta_r L} \frac{1 - e^{(\beta_r - \beta_p)(L+1)}}{1 - e^{(\beta_r - \beta_p)}}.$$

In both cases, the reduction factor can be expressed as

$$(A.4) \quad \frac{\zeta_{\text{multi}}}{\zeta_{\text{single}}} \leq \frac{1}{c} e^{-\min(\beta_p, \beta_r)L} \frac{1 - a^{L+1}}{1 - a},$$

where $a = e^{-|\beta_p - \beta_r|} \in (0, 1)$. Using induction, one can easily show that

$$(A.5) \quad \frac{1 - a^{L+1}}{1 - a} \leq \min\left(L + 1, \frac{1}{1 - a}\right), \quad \forall L \geq 0, \forall a \in (0, 1),$$

which completes the proof for $\beta_p \neq \beta_r$.

For $\beta_p = \beta_r = \min(\beta_p, \beta_r)$, the result of Corollary 4.8 follows trivially from (A.1), since each of the terms in the sum on the right hand side is 1 and $L + 1 < \infty = \frac{1}{1-a}$.

Appendix B. Proof of Corollary 5.5. Due to Corollary 5.2, we have

$$\beta_\ell(\mathbf{v}_\ell^*, \mathbf{v}'_\ell) = \min \left\{ 1, \frac{\pi_\ell(\mathbf{v}'_\ell | \mathbf{y}) \pi_{\ell-1}(\mathbf{v}_{\ell-1}^* | \mathbf{y}) q(\mathbf{v}_{\ell,f}^* | \mathbf{v}'_\ell, \mathbf{v}_{\ell-1}^*)}{\pi_\ell(\mathbf{v}_\ell^* | \mathbf{y}) \pi_{\ell-1}(\mathbf{v}'_{\ell-1} | \mathbf{y}) q(\mathbf{v}'_{\ell,f} | \mathbf{v}_\ell^*, \mathbf{v}'_{\ell-1})} \right\},$$

where, by definition,

$$\frac{\pi_\ell(\mathbf{v}'_\ell | \mathbf{y}) \pi_{\ell-1}(\mathbf{v}_{\ell-1}^* | \mathbf{y})}{\pi_\ell(\mathbf{v}_\ell^* | \mathbf{y}) \pi_{\ell-1}(\mathbf{v}'_{\ell-1} | \mathbf{y})} = \frac{p_\ell(\mathbf{v}'_\ell) p_{\ell-1}(\mathbf{v}_{\ell-1}^*) \exp(-\eta_\ell(\mathbf{v}'_\ell; \mathbf{y}) + \eta_{\ell-1}(\mathbf{v}'_{\ell-1}; \mathbf{y}))}{p_\ell(\mathbf{v}_\ell^*) p_{\ell-1}(\mathbf{v}'_{\ell-1}) \exp(-\eta_\ell(\mathbf{v}_\ell^*; \mathbf{y}) + \eta_{\ell-1}(\mathbf{v}'_{\ell-1}; \mathbf{y}))},$$

such that we can write

$$(B.1) \quad \beta_\ell(\mathbf{v}_\ell^*, \mathbf{v}'_\ell) = \min \left\{ 1, \underbrace{\frac{p_\ell(\mathbf{v}'_\ell) p_{\ell-1}(\mathbf{v}_{\ell-1}^*) q(\mathbf{v}_{\ell,f}^* | \mathbf{v}'_\ell, \mathbf{v}_{\ell-1}^*)}{p_\ell(\mathbf{v}_\ell^*) p_{\ell-1}(\mathbf{v}'_{\ell-1}) q(\mathbf{v}'_{\ell,f} | \mathbf{v}_\ell^*, \mathbf{v}'_{\ell-1})}}_{\textcircled{1}} \underbrace{\frac{\exp(-\eta_\ell(\mathbf{v}'_\ell; \mathbf{y}) + \eta_{\ell-1}(\mathbf{v}'_{\ell-1}; \mathbf{y}))}{\exp(-\eta_\ell(\mathbf{v}_\ell^*; \mathbf{y}) + \eta_{\ell-1}(\mathbf{v}'_{\ell-1}; \mathbf{y}))}}_{\textcircled{2}} \right\}.$$

The level ℓ parameter vectors can be split as $\mathbf{v}'_\ell = (\mathbf{v}'_{\ell,f}, \mathbf{v}'_{\ell,c})$ and $\mathbf{v}_\ell^* = (\mathbf{v}_{\ell,f}^*, \mathbf{v}_{\ell,c}^*)$. and we have $\mathbf{v}'_{\ell,c} = \mathbf{v}'_{\ell-1}$ and $\mathbf{v}_{\ell,c}^* = \mathbf{v}_{\ell-1}^*$ by construction in the coupling procedure. Thus,

$$(B.2) \quad \textcircled{1} = \frac{p_\ell(\mathbf{v}'_{\ell,f}, \mathbf{v}'_{\ell,c}) p_{\ell-1}(\mathbf{v}_{\ell,c}^*) q(\mathbf{v}_{\ell,f}^* | \mathbf{v}'_{\ell,f}, \mathbf{v}'_{\ell,c}, \mathbf{v}_{\ell,c}^*)}{p_\ell(\mathbf{v}_{\ell,f}^*, \mathbf{v}_{\ell,c}^*) p_{\ell-1}(\mathbf{v}'_{\ell,c}) q(\mathbf{v}'_{\ell,f} | \mathbf{v}_{\ell,f}^*, \mathbf{v}_{\ell,c}^*, \mathbf{v}'_{\ell,c})}.$$

The density of the conditional DILI proposal $q(\mathbf{v}'_{\ell,f} | \mathbf{v}_{\ell,f}^*, \mathbf{v}_{\ell,c}^*, \mathbf{v}'_{\ell,c})$ is defined as

$$(B.3) \quad q(\mathbf{v}'_{\ell,f} | \mathbf{v}_{\ell,f}^*, \mathbf{v}_{\ell,c}^*, \mathbf{v}'_{\ell,c}) = \frac{q(\mathbf{v}'_{\ell,f}, \mathbf{v}'_{\ell,c} | \mathbf{v}_{\ell,f}^*, \mathbf{v}_{\ell,c}^*)}{q(\mathbf{v}'_{\ell,c} | \mathbf{v}_{\ell,f}^*, \mathbf{v}_{\ell,c}^*)},$$

that is the ratio between the DILI proposal density and the marginal DILI proposal density,

which takes the form

$$(B.4) \quad q(\mathbf{v}'_{\ell,c} | \mathbf{v}^*_{\ell,f}, \mathbf{v}^*_{\ell,c}) \equiv \int q(\mathbf{v}'_{\ell,f}, \mathbf{v}'_{\ell,c} | \mathbf{v}^*_{\ell,f}, \mathbf{v}^*_{\ell,c}) d\mathbf{v}'_{\ell,f}.$$

Due to Corollary 5.3, the DILI proposal $q(\mathbf{v}'_{\ell} | \mathbf{v}^*_{\ell})$ has the prior distribution $p_{\ell}(\mathbf{v}_{\ell})$ as invariant measure, i.e.,

$$(B.5) \quad p_{\ell}(\mathbf{v}^*_{\ell}) q(\mathbf{v}'_{\ell} | \mathbf{v}^*_{\ell}) = p_{\ell}(\mathbf{v}'_{\ell}).$$

Hence, if $\mathbf{v}^*_{\ell} = (\mathbf{v}^*_{\ell,f}, \mathbf{v}^*_{\ell,c})$ is drawn from the prior $p_{\ell}(\mathbf{v}_{\ell})$, then the proposal candidate $\mathbf{v}'_{\ell} = (\mathbf{v}'_{\ell,f}, \mathbf{v}'_{\ell,c})$ also follows the prior $p_{\ell}(\mathbf{v}_{\ell})$. Furthermore, if \mathbf{v}^*_{ℓ} is drawn from $p_{\ell}(\mathbf{v}_{\ell})$, then the marginal DILI proposal $q(\mathbf{v}'_{\ell,c} | \mathbf{v}^*_{\ell,f}, \mathbf{v}^*_{\ell,c})$ generates candidates with coarse components that follow the marginal prior

$$\int p_{\ell}(\mathbf{v}'_{\ell,f}, \mathbf{v}'_{\ell,c}) d\mathbf{v}'_{\ell,f},$$

which for our particular choice of parametrisation is the same as the prior $p_{\ell-1}(\mathbf{v}'_{\ell,c})$ on level $\ell-1$, that is, $p_{\ell}(\mathbf{v}^*_{\ell}) q(\mathbf{v}'_{\ell,c} | \mathbf{v}^*_{\ell}) = p_{\ell-1}(\mathbf{v}'_{\ell,c})$. Using this identity and substituting (B.3) into (B.2), the ratio ① can be simplified to

$$\begin{aligned} \textcircled{1} &= \frac{p_{\ell}(\mathbf{v}'_{\ell,f}, \mathbf{v}'_{\ell,c}) q(\mathbf{v}^*_{\ell,f}, \mathbf{v}^*_{\ell,c} | \mathbf{v}'_{\ell,f}, \mathbf{v}'_{\ell,c}) q(\mathbf{v}'_{\ell,c} | \mathbf{v}^*_{\ell,f}, \mathbf{v}^*_{\ell,c}) p_{\ell-1}(\mathbf{v}^*_{\ell,c})}{p_{\ell}(\mathbf{v}^*_{\ell,f}, \mathbf{v}^*_{\ell,c}) q(\mathbf{v}'_{\ell,f}, \mathbf{v}'_{\ell,c} | \mathbf{v}^*_{\ell,f}, \mathbf{v}^*_{\ell,c}) q(\mathbf{v}^*_{\ell,c} | \mathbf{v}'_{\ell,f}, \mathbf{v}'_{\ell,c}) p_{\ell-1}(\mathbf{v}'_{\ell,c})} \\ &= \frac{p_{\ell}(\mathbf{v}^*_{\ell,f}, \mathbf{v}^*_{\ell,c}) q(\mathbf{v}'_{\ell,c} | \mathbf{v}^*_{\ell,f}, \mathbf{v}^*_{\ell,c}) p_{\ell-1}(\mathbf{v}^*_{\ell,c})}{p_{\ell}(\mathbf{v}'_{\ell,f}, \mathbf{v}'_{\ell,c}) q(\mathbf{v}^*_{\ell,c} | \mathbf{v}'_{\ell,f}, \mathbf{v}'_{\ell,c}) p_{\ell-1}(\mathbf{v}'_{\ell,c})} = \frac{p_{\ell-1}(\mathbf{v}'_{\ell,c}) p_{\ell-1}(\mathbf{v}^*_{\ell,c})}{p_{\ell-1}(\mathbf{v}^*_{\ell,c}) p_{\ell-1}(\mathbf{v}'_{\ell,c})} = 1. \end{aligned}$$

The result then follows immediately from (B.1).

REFERENCES

- [1] C. ANDRIEU AND E. MOULINES, *On the ergodicity properties of some adaptive MCMC algorithms*, The Annals of Applied Probability, 16 (2006), pp. 1462–1505.
- [2] A. BESKOS, A. JASRA, K. LAW, Y. MARZOUK, AND Y. ZHOU, *Multilevel sequential Monte Carlo with dimension-independent likelihood-informed proposals*, SIAM/ASA Journal on Uncertainty Quantification, 6 (2018), pp. 762–786.
- [3] A. BESKOS, O. PAPASPILIOPOULOS, G. O. ROBERTS, AND P. FEARNHEAD, *Exact and computationally efficient likelihood based estimation for discretely observed diffusion processes (with discussion)*, Journal of the Royal Statistical Society: Series B (Statistical Methodology), 68 (2006), pp. 333–382.
- [4] A. BESKOS, G. O. ROBERTS, A. M. STUART, AND J. VOSS, *MCMC methods for diffusion bridges*, Stochastic Dynamics, 8 (2008), pp. 319–350.
- [5] T. BUI-THANH, O. GHATTAS, J. MARTIN, AND G. STADLER, *A computational framework for infinite-dimensional Bayesian inverse problems. Part I: The linearized case, with application to global seismic inversion*, SIAM Journal on Scientific Computing, 35 (2013), pp. A2494–A2523.
- [6] Y. CHEN, T. A. DAVIS, W. W. HAGER, AND S. RAJAMANICKAM, *Algorithm 887: Cholmod, supernodal sparse cholesky factorization and update/downdate*, PACM Transactions on Mathematical Software, 35 (2008), pp. 22:1–22:14.
- [7] K. CLIFFE, M. GILES, R. SCHEICHL, AND A. TECKENTRUP, *Multilevel Monte Carlo methods and applications to elliptic PDEs with random coefficients*, Computing and Visualization in Science, 14 (2011), pp. 3–15.
- [8] S. L. COTTER, G. O. ROBERTS, A. M. STUART, AND D. WHITE, *MCMC methods for functions: modifying old algorithms to make them faster*, Statistical Science, 28 (2013), pp. 424–446.
- [9] T. CUI, C. FOX, AND M. J. O’SULLIVAN, *Bayesian calibration of a large-scale geothermal reservoir model by a new adaptive delayed acceptance Metropolis Hastings algorithm*, Water Resource Research, 47 (2011), p. W10521.
- [10] T. CUI, K. J. H. LAW, AND Y. M. MARZOUK, *Dimension-independent likelihood-informed MCMC*, Journal of Computational Physics, 304 (2016), pp. 109–137.
- [11] T. CUI, J. MARTIN, Y. M. MARZOUK, A. SOLONEN, AND A. SPANTINI, *Likelihood-informed dimension reduction for nonlinear inverse problems*, Inverse Problems, 30 (2014), p. 114015.
- [12] T. CUI, Y. M. MARZOUK, AND K. E. WILLCOX, *Scalable posterior approximations for large-scale Bayesian*

- inverse problems via likelihood-informed parameter and state reduction*, Journal of Computational Physics, 315 (2016), pp. 363–387.
- [13] T. J. DODWELL, C. KETELSEN, R. SCHEICHL, AND A. L. TECKENTRUP, *A hierarchical multilevel Markov chain Monte Carlo algorithm with applications to uncertainty quantification in subsurface flow*, SIAM/ASA Journal on Uncertainty Quantification, 3 (2015), pp. 1075–1108.
- [14] M. B. GILES, *Multi-level Monte Carlo path simulation*, Operations Research, 56 (2008), pp. 607–617.
- [15] H. HAARIO, M. LAINE, M. LEHTINEN, E. SAKSMAN, AND J. TAMMINEN, *Markov chain Monte Carlo methods for high dimensional inversion in remote sensing*, Journal of the Royal Statistical Society: Series B (Statistical Methodology), 66 (2004), pp. 591–608.
- [16] H. HAARIO, E. SAKSMAN, AND J. TAMMINEN, *An adaptive Metropolis algorithm*, Bernoulli, 7 (2001), pp. 223–242.
- [17] M. HAIRER, A. M. STUART, AND S. VOLLMER, *Spectral gaps for a Metropolis-Hastings algorithm in infinite dimensions*, Annals of Applied Probability, 24 (2014), pp. 2455–2490.
- [18] M. HAIRER, A. M. STUART, AND J. VOSS, *Signal processing problems on function space: Bayesian formulation, stochastic PDEs and effective MCMC methods*, in The Oxford Handbook of Nonlinear Filtering, D. Crisan and B. Rozovsky, eds., Oxford University Press, 2011.
- [19] W. HASTINGS, *Monte Carlo sampling using Markov chains and their applications*, Biometrika, 57 (1970), pp. 97–109.
- [20] D. HIGDON, H. LEE, AND C. HOLLOWMAN, *Markov chain Monte Carlo-based approaches for inference in computationally intensive inverse problems*, in Bayesian Statistics 7, J. M. Bernardo, M. J. Bayarri, J. O. Berger, A. P. Dawid, D. Heckerman, A. F. M. Smith, and M. West, eds., Oxford University Press, 2003, pp. 181–197.
- [21] V. H. HOANG, C. SCHWAB, AND A. M. STUART, *Complexity analysis of accelerated MCMC methods for Bayesian inversion*, Inverse Problems, 29 (2013), p. 085010.
- [22] M. A. IGLESIAS, K. J. H. LAW, AND A. M. STUART, *Evaluation of Gaussian approximations for data assimilation in reservoir models*, Computational Geosciences, 17 (2013), pp. 851–885, <https://doi.org/10.1007/s10596-013-9359-x>.
- [23] A. JASRA, K. KAMATANI, K. J. H. LAW, AND Y. ZHOU, *A multi-index Markov chain Monte Carlo method*, International Journal for Uncertainty Quantification, 8 (2018), pp. 61–73.
- [24] J. P. KAIPIO AND E. SOMERSALO, *Statistical and Computational Inverse Problems*, vol. 160, Springer, New York, 2004.
- [25] K. J. H. LAW, *Proposals which speed up function-space MCMC*, Journal of Computational and Applied Mathematics, 262 (2014), pp. 127–138.
- [26] R. B. LEHOUCQ, D. C. SORENSON, AND C. YANG, *ARPACK Users' Guide.*, Philadelphia, PA: SIAM, 1998.
- [27] J. MARTIN, L. C. WILCOX, C. BURSTEDDE, AND O. GHATTAS, *A stochastic Newton MCMC method for large-scale statistical inverse problems with application to seismic inversion*, SIAM Journal on Scientific Computing, 34 (2012), pp. A1460–A1487.
- [28] N. METROPOLIS, A. W. ROSENBLUTH, M. N. ROSENBLUTH, A. H. TELLER, AND E. TELLER, *Equation of state calculations by fast computing machines*, Journal of Chemical Physics, 21 (1953), pp. 1087–1092.
- [29] N. PETRA, J. MARTIN, G. STADLER, AND O. GHATTAS, *A computational framework for infinite-dimensional Bayesian inverse problems: Part II. Stochastic Newton MCMC with application to ice sheet flow inverse problems*, SIAM Journal on Scientific Computing, 34 (2014), pp. A1525–A1555.
- [30] G. O. ROBERTS AND J. S. ROSENTHAL, *Optimal scaling of discrete approximations to Langevin diffusions*, Journal of the Royal Statistical Society: Series B (Statistical Methodology), 60 (1998), pp. 255–268.
- [31] D. RUDOLF AND B. SPRUNGK, *On a generalization of the preconditioned Crank–Nicolson Metropolis algorithm*, Foundations of Computational Mathematics, 18 (2018), pp. 309–343.
- [32] Y. SAAD, *Numerical methods for large eigenvalue problems: revised edition*, SIAM, 2011.
- [33] A. SPANTINI, A. SOLONEN, T. CUI, J. MARTIN, L. TENORIO, AND Y. M. MARZOUK, *Optimal low-rank approximation of linear Bayesian inverse problems*, SIAM Journal on Scientific Computing, 37 (2015), pp. A2451–A2487.
- [34] A. M. STUART, *Inverse problems: a Bayesian perspective*, Acta Numerica, 19 (2010), pp. 451–559.
- [35] A. TARANTOLA, *Inverse Problem Theory and Methods for Model Parameter Estimation*, Society for Industrial Mathematics, Philadelphia, 2005.
- [36] A. L. TECKENTRUP, R. SCHEICHL, M. B. GILES, AND E. ULLMANN, *Further analysis of multilevel Monte Carlo methods for elliptic PDEs with random coefficients*, Numerische Mathematik, 125 (2013), pp. 569–600.
- [37] L. TIERNEY, *Markov chains for exploring posterior distributions*, Annals of Statistics, 22 (1994), pp. 1701–1728.
- [38] L. TIERNEY, *A note on Metropolis-Hastings kernels for general state spaces*, Annals of Applied Probability, 8 (1998), pp. 1–9.
- [39] O. ZAHM, T. CUI, K. KODY LAW, A. SPANTINI, AND Y. YOUSSEF MARZOUK, *Certified dimension reduction in nonlinear Bayesian inverse problems*, Preprint arXiv:1807.03712, 2018.